Energy Advances

ROYAL SOCIETY OF CHEMISTRY

PERSPECTIVE

View Article Online
View Journal | View Issue

Cite this: *Energy Adv.*, 2024, 3, 2738

Efficiency in photocatalytic production of hydrogen: energetic and sustainability implications

Rocío Sayago-Carro, † Luis José Jiménez-Chavarriga,† Esperanza Fernández-García,† Anna Kubacka* and Marcos Fernández-García *

Received 6th June 2024,
Accepted 1st September 2024

DOI: 10.1039/d4ya00361f

rsc.li/energy-advances

Hydrogen generation through a photocatalytic process appears to be a promising technology to produce this energy vector through a novel, efficient, green, and sustainable process. The fruitful use of sunlight as an excitation source and renewable bio-derived reactants as well as the development of highly efficient catalysts are required to achieve this goal. In this perspective article, we focus on describing how to braid energy and sustainability sides of hydrogen photo-generation into a single parameter, allowing quantitative measurement and trustful comparison of different catalytic systems. Starting from the energy-related efficiency parameters defined by the IUPAC, we present novel approaches leading to parameters enclosing energy and sustainability information. The study is completed with the analysis of other, non-IUPAC, parameters of broad use such as the solar-to-hydrogen observable. The set of results available in the literature for the water splitting reaction and the use of bio-derived sacrificial molecules are reviewed to assess the potential of such reactions in the energy-efficient and sustainable production of hydrogen.

1. Introduction

Hydrogen is a key molecule in many chemical industry processes related to the production of fuels, commodity molecules, and high added value chemicals through hydrogenation reactions and others, and appears as a new energy vector with implications in many new fields including transportation, household and industrial processes. The use of this molecule in such a broad number of chemical processes would be supported by its good properties, in one way or another related to the relatively wide availability on earth due to its huge abundance in terms of mass concerning other elements, its high reactivity and reasonable energy storage capability, as well as the fact that energy release can take place without generating harmful products to the environment or humans. Catalysis and, particularly, photocatalysis can play a role in the hydrogen economy, working on both sides of production and consumption, as part of green and environmentally respectful processes.[1,2]

Photocatalysis uses light to trigger a significant number of chemical reactions and can profit from the use of sunlight as a natural and renewable energy source.[3–5] The setting up of true green processes for hydrogen generation not only requires a renewable energy source but also renewable reactants. Water is a paradigmatic case but if seawater cannot be directly utilized, the massive use of this molecule to produce hydrogen would be detrimental for other uses and hydrogen photo-production would thus compete with water supply for human and agriculture related needs. Also, another critical aspect concerns the physical separation of hydrogen and oxygen, ideally carried out concomitantly with their production, to achieve affordable or competitive cost when compared with the nowadays dominant production from methane reforming and/or the electrolysis of water.[6,7] Alternative molecules generated from bio-based processes can be also good candidates for the massive production of hydrogen. Fermentation derived biomolecules, typically alcohols but also blend with other molecules (like the ABE mixture, *e.g.* acetone, butanol and ethanol), would be thus desirable candidates in the quest of producing renewable hydrogen.[8–11]

A key aspect common to all photocatalytic processes and thus for those aiming to produce hydrogen is the bottleneck derived from the efficiency of the processes.[3–5] Although increasing the always limited efficiency of photocatalytic processes is a must, a previous, seminal question concerns how to define, measure and interpret efficiency. Efficiency is primarily an energy-related parameter associated with any chemical process but a full understanding of the efficiency of a photocatalytic reaction requires including chemical information with

Instituto de Catálisis y Petroleoquímica, CSIC, C/Marie Curie, 2, 28049 Madrid, Spain. E-mail: ak@icp.csic.es, mfg@icp.csic.es

† These authors contribute equally to the work.

implications on sustainability. As a case study, the analysis of the efficiency of the production of hydrogen from alcohols and, generally speaking, carbon-containing molecules, should take into account the evolution of such molecules and the corresponding carbon-containing products generated during reaction. The (carbon-based) product selectivity would have energy-related implications, in this case mainly although not exclusively connected with the consumption of charge carrier species and, in turn, photons during the reaction. Of course, a global understanding of energy related issues requires a full knowledge of the thermodynamics and kinetics of the reaction. On the other hand, as will be shown below, sustainability issues can be connected with the atom selectivity to the target product, in this case hydrogen, as often several hydrogen-containing molecules are produced in the reaction, with the exception of the splitting of water reaction. Other relevant issues for photocatalytic hydrogen production would be connected with environmental and economic issues, also primarily affected by the products generated during the reaction. Although we would not consider in detail these last two due to their limited relationship with the efficiency parameter, it can be noted that the production of hydrogen from waste or the co-production of hydrogen and carbon-containing value added products are research fields with significance in relation to the just mentioned environmental or economic aspects of the process.[5,8]

By analyzing the new perspectives available in the literature, here we will carry out a complete study of the key energy and sustainability related aspects of the reaction in connection with the efficiency of the process. This would provide a holistic view of the measurement and interpretation of the mentioned parameter. In this context, we would note that a survey of literature results suggest, as a first impression, that a rigorous measurement of the efficiency of a light related catalytic process is significantly more complex than that in thermal or classical counterparts. Moreover, there is relatively little information that can allow a real comparison of the performance of photocatalysts coming from different studies. Both facts are intimately linked with the analysis of the light distribution at the reaction medium for any photoreactor configuration as well as for any photocatalytic reaction, and thus for hydrogen production. Measuring and modeling light intensity at a reactor can be carried out at different levels of accuracy mostly as a result of the complex nature of the experimental measurement as well as the computational effort required to achieve an error below experimental uncertainly in the spectral/spatial/directional description of the intensity of light.[12,13] Despite that, the literature presents several parameters that can provide different levels of understanding of the efficiency of a photocatalytic process.[14,15] In fact, a myriad of parameters attempt to measure efficiency, and here we will analyze systematically the most significant ones. The way they are defined and the corresponding experimental/modelling tools required can classify them in a simple way. As outlined above, some of them require the measurement of experimental observables, but in some cases, they also require the above mentioned modeling of the light distribution in the reaction. Rather than showing the mathematical part of the study, the pros and cons as well as the quality of the information extracted from the most representative efficiency parameters for the photocatalytic production of hydrogen will be discussed here. The holistic view attempts to facilitate the progress of the field and to set up the conditions to promote the quantitative measurement of activity in the photocatalytic production of hydrogen and, by extension, for any photocatalytic reaction.

2. Efficiency: energy and sustainability

As efficiency is primarily an energy related parameter, a basic definition comes out from IUPAC recommendations and common sense. Efficiency is described as the ratio between the input and output energy of the reaction, measured joule-to-joule. In photocatalysis, this parameter is dependent on the number of photons, the source of the energy, per unit time (the rate of energy production) involved in the reaction.[16] Work carried out in recent years attempts to provide parameters rendering the real or approximate estimations of efficiency.[13,14,17] Table 1

Table 1 Efficiency parameters defined for hydrogen-production photocatalytic processes

Parameter	Ref.
Efficiency: IUPAC definition η = energy output/energy input	16
Global efficiency of the process $\eta = \eta_{Source}\eta_{reactor}\eta_{reaction}$ η_{Source} = radiant energy (rate of photon generation)/energy input $\eta_{reactor}$ = rate of photon inside the reactor/rate of photon generation $\eta_{reaction} = \eta_{Abs}\eta_{\phi}$ η_{Abs} = rate of photon absorption/rate of photon inside the reactor η_{ϕ} = rate of the target molecule/rate of photon absorption	13, 14, 16 and 17
STH: solar to hydrogen STH = [rate of the target molecule (mol s^{-1}) $\times$ 237 $\times$ 10^3 (J mol^{-1})/P (W m^{-2}) $\times$ A (m^{-2})]	18–20
PTEF: photochemical thermodynamic efficiency factor PTEF = [rate of the primary radical produced ($OH^{\bullet}$)/rate of photon absorption]	21 and 22

summarizes the general formulation of the efficiency in photocatalytic measurements as well as some simple parameters attempting to provide alternative (and more feasible or practical) formulations. A few of the calculations are specific and display wide application within the (sub)field of hydrogen production. Note that Table 1 collects parameters expressed as a fraction (of unity), although parallel formulations can be presented in percentage ($\times 100$).

2.1. Global efficiency

The global efficiency of a photoreaction reaction (second row of Table 1) can be defined conceptually as composed of three different terms. Each term can have an associated parameter. They define the different parts of the process to extract a rational interpretation of the losses taking place and thus to provide a complete answer to the interpretation of the efficiency. A first point to note is that some of these parameters can be calculated or approximated by a single parameter and, as said, can be estimated using different degrees of approximation.

The first term of the global efficiency is η_{Source}. If the energy source is the sun, we can consider that this parameter would take the unit value although the analysis of the ''efficiency'' in collecting sunlight at a reactor using parabolic or other concentrators would provide a different value.[23] If an artificial source is utilized, the efficiency is always below 1 and depends primarily on the type of lamp. Obviously, LED lamps would have higher efficiency than mercury or xenon lamps as they have lower heat losses. Complete information about how to calculate this factor using artificial sources within the context of a photocatalytic process can be found in ref. 24–28.

The second term concerns the reactor under illumination, η_{reactor}. Sometimes it is called the reactor radiation incidence efficiency. Measuring (experimentally) the photons at each point of a reactor cannot be accounted for under most experimental conditions as the light-measurement equipment will interfere with light, cannot be physically allocated at the reactor, and/or the corresponding measurement cannot achieve adequate spatial discrimination. Moreover, if the dispersion of light is a relevant contribution to the mater–light interaction process, light intensity at any point of a reactor is intimately associated with the catalyst presence at the reaction medium. In brief, from a practical point of view, this term corresponds to a loss term mainly associated with the radiation losses taking place through all the walls of the reactor. On occasions, the coupling of $\eta_{\text{reactor}} \times \eta_{\text{Abs}}$ is the one calculated and reported. For some of the IUPAC definitions, such as the photonic yield, the experimental measurement of light intensity, or more properly, the number of photons per unit time, behind the illuminated reactor wall/window(s) is required.[16] So, not all radiation losses will be accounted for while using the IUPAC defined parameter. The light intensity after the corresponding wall/window (the one illuminated) is, on the other hand, a boundary condition included in the calculation of the last term presented in the global efficiency, η_{reaction}.[12,13] As it is obvious, η_{reactor} cannot achieve a unity value. The corresponding value depends primarily on the geometry of illumination and reactor configuration but also on catalyst concentration and physicochemical properties.

Most of the literature concerns the calculation of the η_{reaction} term. As the central piece of the formulation, this term contains the calculation of the so-called ''quantum efficiency'' of the process, η_{ϕ}. Rigorously, the parameter requires measurement/calculation of the rate of reaction and the rate of photon absorption. The difficulty in providing an accurate value for the last parameter leads to different ways of calculation as well as the use of alternative parameters substituting it. In this context, we stress the fact that illumination in a photocatalytic reactor is carried out using multi-wavelength sources. This is the case of sunlight and also of artificial light sources with reasonable light intensity. Other valuable experiments with relatively poor control of hydrodynamic conditions (using reaction chambers rather than reactors) and/or model conditions can use monochromatic, laser-type sources. The multi-wavelength nature of the source of interest defines the way the quantum efficiency parameter is calculated in photocatalysis and here utilized. Nevertheless, parallel definitions are available for efficiency parameters measuring η_{reaction} for monochromatic light sources.[16]

So, through the need of obtaining the rate of photon absorption, the rigorous calculation of the quantum efficiency requires careful measurement of the boundary conditions using actinometry and/or radiometry and the use of numerical procedures to obtain the intensity of light at each point of the reactor. The rate of photon absorption is the product of the absorption coefficient of the catalyst multiplied by the intensity of light at each point of the reactor. The interaction of light with matter in a photocatalytic reactor defines two types of systems. The first one is called pseudo-homogeneous and typically corresponds to suspended solids. Dispersion of light plays a key role although is not the single light–matter effect of relevance as absorption, reflection and refraction of light should be considered. Three methods are the most popular to obtain the rate of photon absorption through the solving of the integro-differential radiative transfer equation. These are the discrete ordinate method, the finite volume method and the Monte Carlo method. They are exact as far as true convergence is obtained in the spectral/spatial/directional representation of light at the reactor. As they all imply intensive computational effort, more simple methods taking advantage of a limited representation(s) of the directional properties of light at the reactor or other simplifications have been implemented. These methods facilitate the solving of the integro-differential radiative transfer equation through the use of (semi-) closed (analytical) formulae instead of the use of numerical (accurate) tools.[12,13,29] New methods recently proposed in the literature used machine learning and literature results to set up alternative procedures to calculate η_{reaction} without detailed analysis of the light–matter interaction taking place under reaction conditions. They provide an alternative way of measuring η_{reaction} to the one presented in Table 1, although the results show that similar observables as the rate of photon absorption should be utilized in order to provide meaningful results.[30] The second type of system is called

heterogeneous and the main light–matter events are absorption/transmittance, reflection and refraction. They mostly relate to supported catalysts although some systems specifically designed for multiple scattering (like photonic materials) would not be considered ''heterogeneous''. In any case, here the relevant optical properties of the solids and the rate of photon absorption are obtained with the help of experimental measurements of the above mentioned optical properties and boundary conditions and the application of classical optics.[12,13,23]

As will be shown hereafter, for hydrogen photo-production, water splitting reports display relatively low values (except for tests using monochromatic sources) of the efficiency parameters. Higher values are typically encountered for the production of hydrogen using sacrificial molecules. In any case, realistic calculations would lead to a value below 0.3–0.2 in the best cases. Considering that η_{Source} could be considered unity for the best case but η_{reactor} has inherent losses for all configurations reported and thus a value below unity, the maximum (true) efficiency reported would never exceed 0.3 or 30%. This appears to be a reasonable upper bound limit. Values reported above this point would suffer from severe simplifications, in most cases associated with the analysis of the relevant properties of the illumination source. These typically concern (i) the handling of the total photon flux of the light source as monochromatic (using a central wavenumber which, even using filters, is incorrect); (ii) the use of the nominal power of the source or a simple evaluation of the radiation field intensity; and/or (iii) restriction of the radiation–catalyst interaction model to absorption events.

For our purposes, a critical issue, connected with the (not so obvious) relationship in the sustainability of the chemical process, comes out from the dimensionality of the quantum efficiency parameter as defined in Table 1. The physical units of the parameter are mole of the target molecule per mole (Einstein) of photons. To provide a dimensionless efficiency parameter, the so-called ''selectivity'' factor should be included in the denominator of η_ϕ. The new efficiency parameter is called the fraction of useful photons, η_Θ. Such a parameter uses the selectivity factor ($S = \sum n_i S_i$) that can be calculated as the summation (calculated, i, on the basis of the molecule utilized to measure the reaction rate present at the numerator of the efficiency parameter, in our case, hydrogen) over all products of the reaction of the inverse of the number of charge carrier species (n_i) involved in the generation of the product multiplied by its fractional selectivity (S_i). Considering that one photon is used to generate one (electron–hole) charge carrier pair, the units of the selectivity factor are mole of the target molecule per Einstein of photons.[13] Through the selectivity factor, the inclusion of chemical information in the quantum efficiency parameter leads to a new dimensionless parameter that allows measuring the real fraction of the (initial) photons involved in the reaction. It takes into account the fact that the different products of a reaction consume a different number of charge carrier species and in turn photons. This is easily visualized considering that the oxidation or the reduction of a chemical species can progress with the formation of different products. For example, in the case of a sacrificial molecule utilized for hydrogen production, the oxidation of the molecule would progress up to carbon dioxide through several intermediates usually containing a higher proportion of oxygen than the initial molecule. As shown later in this work, as there is a univocal correlation between the number of charge carrier species and the production of hydrogen, the fraction of useful photons also provides the ground for a measure of the sustainability of the reaction through the relationship with the atom efficiency on a hydrogen basis.

2.2. Other parameters

A second point to mention in the context of analyzing η_ϕ is the formulation of alternative parameters that would be easier to obtain and would substitute the quantum efficiency parameter. For polychromatic sources, the IUPAC defines the so-called ''quantum yield'' for this purpose. As mentioned, such a definition eliminates the calculation of the rate of photon absorption in η_ϕ and utilizes the rate of incident photons inside the irradiated window of the reactor.[16] So, instead of using the absorbed photons, the quantum yield uses the impinging photons once the reactor losses are considered in a first approximation (radiation losses inherent to the illuminated but not all walls of the reactor). A trivial inspection of Table 1 indicates that this parameter would not allow obtaining a meaningful value for the (global) efficiency, η, of the process but can serve as a guide to estimate η_{reaction}. As trivially deduced from its definition, the photonic yield renders a lower bound to the accurate calculation (*e.g.* using the quantum efficiency) of η_{reaction}. Note however that a significant number of reports do not use the IUPAC definition(s) to report efficiency and typically use the total incident photon flux (instead of the rate of photon absorption or the photon flux inside the irradiated window) to provide a different parameter, commonly called ''apparent quantum efficiency'' or by the IUPAC ''apparent (photonic) yield''. This parameter, not included in Table 1, is obsolete according to the IUPAC. Nevertheless, due to its broad use, we will collect information in the following section(s) using such parameters.[16]

In the way to provide simple estimations of the efficiency and thus to avoid the complex experimental-modeling methodologies required for accurate estimation, other simple parameters have been implemented by several authors. The most popular by far is the so-called solar-to-hydrogen STH parameter. The parameter measures the chemical energy of the hydrogen produced *vs.* the incident sunlight energy. The incident energy is referenced to the Air Mass 1.5 Global (AM 1.5G; 100 mW cm^{-2}) standard. Although initially developed for (photo)electrochemical methods, the application of STH as collected in Table 1 has been utilized by many authors in the photocatalysis field.[18–20] STH is a parameter originally designed for the pure water splitting reaction, but the literature shows its use for reactions utilizing sacrificial agents. The maximum value would depend on the solar range (source) to be used. If the UV/visible/IR component is the target source, the maximum of the parameter is around *ca.* 3.3/43/53%. Of course, the sun

provides IR photons at sea level up to *ca.* 2500 nm (in fact, up to 1800 nm as CO_2/water essentially absorbs all photons above such cut-off), but no single material is able to use (relatively) low energy photons. Likely, the harvesting of nearIR photons up to the cut-off energy just mentioned would require the participation of carbonaceous-type materials and/or lanthanides with engineering f-electron subshells. These options appear to be able to profit from the solar spectrum up to a wavelength of *ca.* 1150 nm (1.08 eV). An additional option for the future could be the use of double-photon technologies but nowadays these are rather inefficient and typically utilize rather toxic and/or unstable (under reaction conditions) materials.[31] From the above discussion, a target value of 10% requires the use of the visible and/or the nearIR contributions of sunlight and, if the profit is limited to *ca.* 1150 nm, top values above 65–70% are unattainable. Such a maximum does not consider any type of loss and thus is an upper bound.

Considering the interpretation of the STH observable, a key point, repeatedly mentioned in the literature, is that the useful range of the solar spectrum utilized in the photocatalytic process depends primarily on the band gap energy of the catalyst and there is no direct or straightforward way of introducing such information into the STH parameter. In fact, the STH parameter is a kind of black box, as the losses cannot be associated with confidence with any physical parameter of the reactor or the reaction (including the photocatalyst) that would allow the optimization of the process. As mentioned before, the adequate measure of the effects of light absorption under reaction conditions can be only achieved through the rate of photon absorption or equivalent formulations and, in general, the full knowledge of the $\eta_{Source}\eta_{reactor}\eta_{reaction}$ efficiencies is required. Nevertheless, the strongest point of the STH parameter comes out from the relatively easy calculation of the maximum achievable for a specific material (primarily defined by the band gap energy) as well as its wide application. Valuable tests for different reactor configurations and semiconductors with different band gap energies covering the UV, visible and nearIR ranges have been presented in the literature.[32,33]

As a representative example of other useful parameters of relatively limited application for measuring efficiency in hydrogen production, we can present the so-called ''photochemical thermodynamic efficiency'' factor. Table 1 shows that this parameter replaces, in the formulae of the quantum efficiency, the rate of target molecule production by the rate of formation of the primary radical involved (for our purposes, hydrogen production, hydroxyl type radicals). The parameter will thus provide a way to measure the ratio of the energy consumed in the reaction *vs.* the input energy. Depending on the path for hydroxyl generation, the maximum PTEF achieved can be different. In the absence of oxygen, hydroxyl radicals can be formed exclusively from holes and a unity value appears as the maximum value. In the presence of oxygen, the maximum value can be up to 1.3.[21,22]

3. Production of hydrogen: efficiency

Once the different efficiency parameters were presented and their interpretation discussed, we will review the literature data. To this end, we will present data corresponding to water splitting as well as the reforming type reactions taking place with the help of most frequently used sacrificial agents such as alcohols, acids, sugars and others. Some reports provide information concerning several sacrificial molecules and are considered separately for each case included in the study. The summary of the literature attempts to illustrate the dual (energy but also sustainability related) information enclosed in the studies reported. This implies that the perspective article focuses attention on two types of studies. First, we selected works carrying out the analysis of light intensity at the reactor to report the IUPAC recommended parameters and/or the analysis of efficiency parameters presented in Table 1. Second, other works are selected as they provide a complete report about the selectivity of the reaction when sacrificial agents are used. Although the set of results presented may not provide a complete view of the field of the photocatalytic production of hydrogen, it is ideally suited to sustain the analysis of the efficiency of the reaction in terms of energy and sustainability issues. In this context, we note that full information about the different catalyst formulations and characteristics is available in many review articles, such as those described in the introduction section.[3,4,6,8–11]

For each ''type of'' substrate (water, carbon-containing molecules) mentioned, we summarize the relevant information in two tables enclosing the information of the efficiency and, when required and/or available, the selectivity of the reaction. Concerning the efficiency, we summarize results considering five–six different parameters encountered in the literature. Here such results are defined in terms of the mathematical process utilized rather than the efficiency parameters claimed to be calculated by the authors. These are the (i) quantum efficiency (QE) and (ii) photonic yield (PY) parameters reported in publications following the IUPAC recipes, as discussed in the previous section. Connected with the QE parameter we also investigated (iii) the fraction of useful photons. We also summarized data considering (iv) the apparent (photonic) yield (APY), calculated using the incident photon flux in the denominator of the efficiency parameter. As mentioned in the previous section, this is frequently called by certain authors as apparent quantum efficiency. Finally, the (v) solar-to-hydrogen (STH) and (vi) photochemical thermodynamic efficiency factor (PTEP) parameters are presented as defined in Table 1. A general point is that most of the quantum efficiency, photonic yield or apparent photonic yield data are calculated using a factor 2 multiplying the reaction rate. Although the authors may not be aware, this constant is the selectivity factor for the photocatalytic generation of hydrogen. Thus, in the case of quantum efficiency, the reported parameter is, in fact, the dimensionless ''fraction of useful photons''. In the other four parameters, the introduction of this factor is relatively meaningless although may find ground through the parallelism with the quantum efficiency. We will further discuss these points and their implications in subsequent paragraphs. Finally, a summary of the relevant information for the most studied reactions is depicted in an associated figure. This figure attempts to summarize the information of charge carrier species as well as the

Table 2 Summary of efficiency values presented in the literature for the water splitting reaction[34–48]

Catalyst	Source and Radiation	Reaction conditions reagent/catalyst concentration	QE, PY, APY, STH, PTEF/%	Ref.
0.1 wt% Ru-CrO_x/$SrTiO_3$:Al	Sunlight	H_2O	0.76	35
1 wt% Ru/$SrTiO_3$:Rh	Xe lamp (300 W) 420–440 nm	H_2O 0.42 g L^{-1}	5.9 0.10	36
Ru/$SrTiO_3$:La,Rh	Xe lamp (300 W) >420 nm	H_2O 0.25 g L^{-1}	3.3 1.10	37
4 mol% Ru/$SrTiO_3$:La, 4 mol% Rh/C/$BiVO_4$:0.05 mol% Mo	Xe lamp (300 W) >420 nm	H_2O 0.25 g L^{-1}	0.7 1.0	38
0.3 wt% Pt/$SrTiO_3$:1 mol% Cr/1 mol% Ta	Xe lamp (300 W) >420 nm	H_2O 0.80 g L^{-1}	0.10	39
0.75 wt% Ni–$La_2Ti_2O_7$:8 mol% Ba	Hg lamp (450 W) >420 nm	H_2O 2 g L^{-1}	50.0	40
Cr_2O_3/Rh/$La_5Ti_2Cu_{0.9}Ag_{0.1}S_5O_7$:Ga	Xe lamp 300 W 420 nm	H_2O 0.07 g L^{-1}	4.9 0.11	41
0.3 wt% Pt/TaON	Xe lamp (300 W) >420 nm	H_2O	0.4%	42
1.0 wt% Pt/ZrO_2/TaON	Xe lamp (300 W) >420 nm	H_2O 0.50 g L^{-1}	6.30	43
g-C_3N_4	Xe lamp 300 W >420 nm	H_2O 0.50 g L^{-1}	1.4 0.06	44
Pt/g-C_3N_4	Xe lamp (300 W) 390–700 nm	H_2O 0.30 g L^{-1}	1.5	45
5 wt% Pt@βKetone COF	Xe lamp (300 W) >420 nm	H_2O 0.30 g L^{-1}	2.8 23.0	34
0.1 wt% Rh-0.1 wt% CrO_x/ $SrTiO_3$:Al	Xe lamp (300 W) 365 nm	H_2O 0.20 g L^{-1}	65.0 10.0	46
0.1 wt% Rh-0.05 wt% Cr_2O_3/ 0.05 wt% CoOOH/$SrTiO_3$Al	Xe lamp 300 W 365 nm	H_2O	91.6 0.065	47
0.05 wt% NiO–$NaTaO_3$	Xe lamp (300 W) 270 nm	H_2O 2.9 g L^{-1}	20.0	48

evolution of the reactants under reaction conditions. With the complete picture of the process, we would have the basis to rationalize the literature results reporting the efficiency of the photocatalytic process in terms of energy and sustainability issues.

3.1. Water

For the case of water splitting, Table 2 collects the data of efficiency. Of course, selectivity issues are trivial as hydrogen is the only possible product containing hydrogen atoms. Typical systems tested are composite systems based on oxides, oxysulfides, oxynitrides, nitrides and carbon nitride. As well described in the literature, such catalysts work under different Z-scheme type schemes allowing efficient charge carrier species separation and semi-reactions for hole and electron species at separated surface sites.[3,19,20] Although the results using monochromatic sources (the 3 entries listed at the end of Table 2) can reach high values, when attempting to profit from the whole visible range, performance is significantly affected. Under polychromatic excitation, note that some values reported in the table and using the apparent yield/quantum efficiency (APY) are relatively high. This would likely indicate that the simple way of measuring efficiency is not only obsolete, as dictated by the IUPAC, but likely would lead to unphysical values in a significant number of cases. The STH values provided are always below or around 1%. Only in the case of a platinum promoted COF, we find a value exceeding the above mentioned cut-off.[34] Despite this, for a realistic test, using a

Table 3 Summary of efficiency values presented in the literature for hydrogen production using methanol as a sacrificial agent[49–78]

Catalyst	Source and radiation	Reaction conditions sacrificial agent/catalyst concentration	QE, PY, APY, STH, PTEF/%	Ref.
TiO_2	Two solarium Philips HB 175 lamps. 4 × 15 W Philips CLEO fluorescent lamps 300–400 nm (max. 365 nm)	Methanol:H_2O 1:4 1 g L^{-1}	2.18	50
TiO_2 (P25)	8-W Hg UVA lamp 365 nm	Methanol:H_2O 1:1 0.25 g L^{-1} Opt.	1.0	51
0.5 wt%Pt/TiO_2(P25)	Hg–Xe lamp (500 W) 280–400 nm	Methanol:H_2O 1:1 0.50 g L^{-1} Opt.	28	52
2.1 wt% Pt/TiO_2	Philips CLEO 15W fluorescent lamps 300–400 nm (max.365 nm)	Methanol:H2O 1:4 1 g L^{-1}	31.8	53
1 wt% Pt/TiO_2 nanotubes	High pressure Xe/Hg lamp 150 W 313 nm	Methanol:H_2O 1:3.5	16.0	54
0.64 wt% Pt/TiO_2	UV-vis 150W Xe lamp >420 nm	Gas phase from a methanol:H_2O liquid mixture 1:5	14.0	55
1 wt% Cu/TiO_2	Xe lamp (300 W) 365 nm	Methanol:H_2O 1:1 1 g L^{-1}	10.0	56
0.5 wt% PtCu/TiO_2	LED irradiation 365 nm (70 °C)	Methanol:H_2O 3:7 0.13 g L^{-1}	99.2	57
0.8 wt% Au/TiO_2	3 Solarium Philips B175 lamps, each equipped with 4 15 W Philips CLEO fluorescent lamps 300–400 nm (max. 365 nm)	Methanol:H_2O 1:4 1 g L^{-1}	17.5	58
1.5 wt% Au/TiO_2	Two Solarium Philips HB 175 lamps. 4 × 15 W Philips CLEO fluorescent Lamps 300–400 nm (max. 365 nm)	Methanol:H_2O 1:4 1 g L^{-1}	2.6	59
1 wt% Pt/0.5 mol% SnS_2–TiO_2	Hg–Xe lamp (500 W) 280-400 nm	Methanol:H_2O 3:7 0.50 g L^{-1} Opt.	4.3	60
1 wt% Pt/(Nb)TiO_2	Hg–Xe lamp (500 W) 280–400nm 420–680 nm	Methanol:H_2O 3:7 0.50 g L^{-1} Opt.	UV: 5.0 Visible: 2.5	61
1 wt%Pt/0.25 mol% $NbTiO_2$	Hg–Xe lamp (500W) 280–400nm 420–680 nm	Methanol:H_2O 3:7 0.50 g L^{-1} Opt.	UV: 6.5 Visible: 3.0	62
1Pt–Pd/(1:1)/(3mol%Nb)TiO_2	Xe lamp (500 W) 280–400nm 420–680 nm	Methanol:H_2O 3:7 0.50 g L^{-1} Opt.	UV: 2.7 Vis: 1.0	63
1 wt% Au/1.75 mol% Zr–TiO_2	Xe lamp (500 W) 280–400nm 420–680 nm	Methanol:H_2O 3:7 0.50 g L^{-1} Opt.	UV: 3.3 Vis: 1.9	64
0.23 wt% $Ni(OH)_2$/TiO_2	Four low power UV-LEDs 3 W; 80.0 mW cm^{-2} 365 nm	Methanol:H_2O 1:3 0.63 g L^{-1}	12.4	65
2 wt% NiO/TiO_2	8W Hg lamp 254 nm	Methanol:H_2O 1:1 1 g L^{-1}	2.9	66
0.25 wt% NiO/TiO_2	Xe lamp (300 W), 25 mW cm^{-2} 365 nm	Methanol:H_2O 1:4 0.63 g L^{-1}	1.7	67
1 wt% Pt/1.0 mol% SnS_x-2.5 mol% Zr–TiO_2	500 W Xe arc lamp (Lot Oriel) 280–400 nm	Methanol:H_2O 3:7 0.50 g L^{-1} Opt.	15.7	68
1 wt% Pt/3–5 mol%($CuGaS_2$)–TiO_2	Hg–Xe lamp (500 W) 280–400nm 420–680 nm	Methanol:H_2O 3:7 0.50 g L^{-1} Opt.	UV: 5.1 Vis: 5.8	49
0.5 wt% Cr_2O_3/1.0 wt% Pt/0.5 wt% IrO_2/STOS	Xe lamp 300W 420 nm	Methanol:H_2O 1:10 1.3 g L^{-1} Opt.	21.7 0.22	69
0.01 wt% Pd/TiO_2–WO_3	Xe lamp (300 W) 300–800 nm 300–400 nm	Methanol:H_2O 1:1 0.17 g L^{-1} Opt.	2.3 7.7	70
Au@Cu_7S_4	Monochromatic Xe lamp (150 W) monochromator 500–2200 nm	Methanol:H_2O 1:20	9.4 7.3	71
$ZnIn_2S_4$	420 nm	Methanol:H_2O 1:4 0.7 g L^{-1}	5.8	72
MoS_2/CdS nanorods	Xe lamp (300 W)	Methanol:H_2O 4:1 2 g L^{-1}	5.0	73
$ZnIn_2S_4$/$ZnWO_x$	Xe lamp (300 W) >420 nm	Methanol:H_2O	10.5	74
InGaN/GaN	Xe lamp (300 W) 395–405 nm 440–450 nm	Methanol:H_2O 1:10	1.9 13.0	75
GaN:ZnO	Xe lamp (300 W) >420 nm	Methanol:H2O 1:9 0.25 g L^{-1}	5.1	76
1 wt% Pt/g-C_3N_4 nanotube	Xe lamp (300 W) >420 nm	Methanol:H_2O 1:3 1.3 g L^{-1}	5.7	77
Graphene-like dot/N-defective g-C_3N_4	Xe lamp (300 W) 420–800 nm	Methanol:H_2O 1:3 1 g L^{-1}	13.0	78

100 m^2 surface exposed to sunlight during a long period of time, the group of Domen obtained a 0.76% value for the STH parameter (1st entry of Table 2).[35] The absence of information considering the measurement of the quantum efficiency can be

Table 4 Summary of selectivity values presented in the literature for hydrogen production using methanol as a sacrificial agent[50,53,57,58,61,78–82]

Catalyst	Source and radiation	Reaction conditions reagent/catalyst concentration	Product	Selectivity C basis/%	Selectivity H basis/%	Ref.
TiO_2	Two Solarium Philips HB 175 lamps. 4 × 15 W Philips CLEO Fluorescent lamps 300–400 nm (max. 365 nm)	Methanol:H_2O 1:4 1 g L^{-1}	HCHO	100	100	50
TiO_2 1 wt% Au/TiO_2 1 wt% Pt/TiO_2	Xe lamp (300 W)	Gas phase from a methanol:H_2O liquid mixture 1:5	TiO_2 H_2 H_2CO CO CO_2 Au/TiO_2 H_2 H_2CO CO CO_2 Pt/TiO_2 H_2 H_2CO CO CO_2	 — 52.6 31.6 15.8 — 72.3 2.9 24.8 — 61.2 1.6 37.2	 86.7 13.3 — — 72.8 27.2 — — 79.8 20.2 — —	55
1wt% Pt/(Nb)TiO_2	Hg–Xe lamp (500 W) UV: 280–400nm Vis.: 420–680 nm	Methanol:H_2O 3:7 0.50 g L^{-1} Opt.	Pt/TiO_2 UV H_2 HCOOH $HCOOCH_3$ Vis H_2 HCOOH $HCOOCH_3$ Pt/(Nb)TiO_2 UV H_2 HCOOH HCHO $HCOOCH_3$ Vis H_2 HCOOH $HCOOCH_3$	 — 90 10 — 98 2 — 85 8 7 — 90 10	 78.4 17.7 13.9 79.7 17.6 0.8 79.0 18.5 1.7 0.8 78.4 17.6 3.9	61
2.1 wt% Pt/TiO_2	Philips CLEO 15W fluorescent lamps 300–400 nm (max. 365 nm)	Methanol:H_2O 1:4 1 g L^{-1}	H_2 HCHO HCOOH	— 96.8 3.2	50.8 47.7 1.5	53
0.5 wt% Pt/TiO_2	Hg lamp (250 W) 350–450 nm	Gas phase from a methanol:H_2O liquid mixture 1:5	H_2 HCHO HCOOH CO_2	— 78.2 1.9 19.9	77.2 22.3 0.5 —	80
10wt% Pt/P25	Xe lamp (300 W)	Methanol:H_2O 1:5 15 g L^{-1}	H_2 HCHO HCOOH CH_4 CO CO_2	— 0.2 27.6 7.8 6.2 56.2	88.1 0.8 11.1 1.3 — —	79
1.0 wt% Pt/TiO_2	Xe lamp (1000 W)	Methanol:H_2O 1:10 0.5 g L^{-1}	H_2 HCHO HCOOH CO CO_2	— 63.9 13.6 7.4 15.1	66.9 27.3 5.8 — —	81
0.8 wt% Au/TiO_2	3 Solarium Philips B175 lamps, each equipped with 4 15 W Philips CLEO fluorescent lamps 300–400 nm (max. 365 nm)	Methanol:H_2O 1:4 1 g L^{-1}	H_2 HCHO HCOOH	— 58.1 41.9	58.7 24.0 17.3	58
0.5 wt% PtCu/Ti O_2	LED irradiation 365 nm (70 °C)	Methanol:H_2O 3:7 0.13 g L^{-1}	H_2 HCHO CO	 98.6 0.06	66.7 33.3 0	57
5 wt% Cu/CeO_2	Xe lamp (300 W)	Methanol/H_2O 1:1	H_2 CO CO_2	100 0 100	100 0 100	82
Graphene-like dot/N-defective g-C_3N_4	Xe lamp (300 W) 420–800 nm	Methanol:H_2O 1:3 1 g L^{-1}	H_2 CO CO_2 CH_4	0 2.7 96.5 0.2	99.7 0 0 0.3	78

noticed and thus the potential of the tested systems would need to be further assessed. Nevertheless, it can be concluded that the current status of water splitting is far from reaching the objective of using 10% of the sunlight energy.

3.2. Methanol

Methanol is selected as the initial carbon-containing sacrificial molecule here studied. It corresponds to the case more broadly studied. Also, the relative simplicity of the molecule allows for tracking all (carbon, oxygen and hydrogen containing) products potentially produced under reaction conditions. The summary of efficiency values reported is presented in Table 3. In this table, we selected as initial entries titania-based systems, promoted with Pt and other (noble and non-noble) co-catalysts as well as those systems obtained through doping of titania and/or composites with a dominant presence of the mentioned oxide. The corresponding results included in Table 3 are followed by other systems based on other oxides and thus other semiconductors, mostly sulfides and carbon nitride. Very high values are typically encountered when using the apparent photonic yield (APY), also called the apparent quantum yield. This has been commented already for the table considering water splitting results. The titania-based systems are reported mostly under UV irradiation and, in some cases, under visible irradiation. Efficiency under visible light is always inferior except for cases concerning composite systems where a second semiconductor is specifically devised for it. In any case, for the complete UV-visible range of sunlight (*ca.* 280–760 nm), all systems display an efficiency below *ca.* 6–7% (maximum achieved to our knowledge in ref. 49). Higher values can be encountered under UV illumination. The maximum of 6–7% could be achieved with other systems like carbon nitride, $ZnIn_2S_4$-based, or doped GaN systems (last entries of Table 3), although the absence of accurate calculations of the quantum efficiency does not allow one to establish this point with confidence for non-titania based systems. On the other hand, Table 3 would indicate the limited use of the STH or other non-IUPAC parameters when methanol is utilized to generate hydrogen. In summary, it can be considered that the best systems could be close to a real efficiency of 10% in the UV-visible range. Likely, the titania-based and other systems listed in Table 3 would not use efficiently the nearIR range, and thus there is room to improve and achieve efficient use of the sunlight full spectrum. A point to remark again is, however, that the energy release of all photons is not the same and although the nearIR range is very important, its energy content is significantly lower as well as more problematic to be used than that corresponding to the visible range, as already mentioned in the previous section.

Interestingly, measuring the hydrogen generation from methanol using the quantum efficiency cannot take into account explicitly the number of charge carrier species utilized. Neither can it include chemical information. However, the photocatalytic reaction triggers the formation of a significant number of carbon, oxygen and hydrogen-containing molecules, with direct consequences in the production of hydrogen. This comes out for the presence of hydrogen in such molecules, limiting the production of molecular hydrogen. Table 4 captures the most relevant works where the selectivity of the reaction has been explored and reported. It contains information of the selectivity on carbon and hydrogen atomic bases. Due to the relative simplicity of the reactant(s), methanol and water, all potential products of the reactions have been reported if considered the works previoulsy reported collectively. The summary of the evolution of the reactants and the concomitant production of hydrogen is presented in Fig. 1. Under illumination, after charge separation and creation of electron–hole pairs, two different radicals would be formed

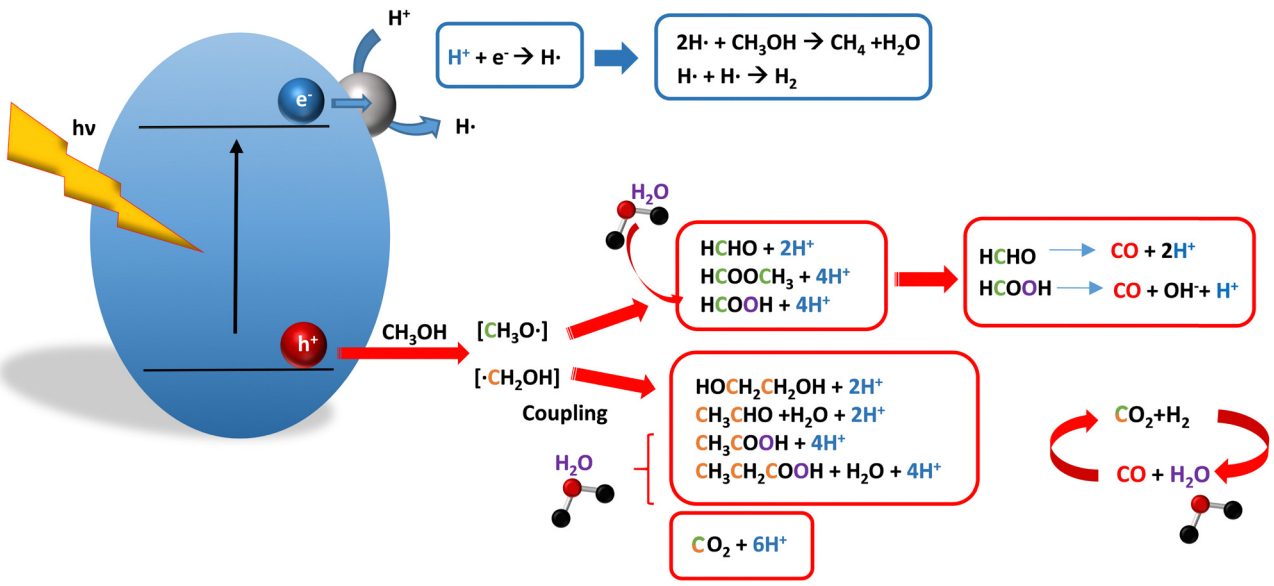

Fig. 1 Schematic representation of the radical species and intermediates detected in the photocatalytic production using methanol as a sacrificial molecule. Colour codes are explained in the text.

from the hole-related species attack on the sacrificial molecule. The most typical products are related to the initial production of an oxygen-type radical generated by the mentioned hole-type attack on the OH moiety, leading to an oxygen-centered alkoxy-type radical. This radical is highlighted with a green colour in Fig. 1. The subsequent (further) radical attack by hole-type species renders the carbon-containing oxidized species as well as protons. In a chain-type mechanism, formaldehyde, formic acid and carbon dioxide would be formed. It is important to note that formaldehyde is formed in a dehydrogenation step while the formation of the next intermediate, formic acid, involves water in a reforming-type step. This point is highlighted using a magenta colour for an oxygen atom in Fig. 1. To generate this (and subsequent) intermediates, protons are extracted from the two reactant molecules (although we did not use the magenta colour in carbon dioxide and other molecules generated from the acid intermediate and included in Fig. 1).[55,61,79] Formation of carbon dioxide can be considered as a final step of the chain-type mechanism, but decarbonylation steps and production of carbon monoxide with subsequent triggering of the water gas shift reaction have been also shown to be involved in the reaction. In addition, coupling of methanol molecules activated through the alkoxy route can lead to the formation of methyl formate species.[78,79] As said, each step generates concomitantly hydrogen ions consuming the hole-type radicals in a one-by-one ratio. The number of hole-type charge carrier/hydrogen ions is counted using the last observable in Fig. 1. This information is key to obtaining the selectivity factor. In addition to this path, the formation of a carbon-centered radical (highlighted with an orange colour in Fig. 1) can also take place, generating through a coupling step, as a first intermediate, ethylene glycol, a C_2 molecule. The further evolution of ethylene glycol leads to other C_2 molecules as well as C_3 molecules formed with methanol molecules activated using exclusively the carbon-centered route or, in specific C_{2+} cases, a mixture of the paths. In subsequent steps, it is obvious that this (carbon-centered radical) route can also lead to C_1 products including carbon dioxides.[68,73] Again, we remark that formation of the (acetic) acid intermediate requires the use of water, as indicated in Fig. 1. In all cases (see the upper part of Fig. 1), the generation of the hydrogen molecule takes place from the hydrogen ions concomitantly originated with the carbon-containing intermediates and electrons, closing the catalytic cycle. Nevertheless, the presence of products which compete for the electrons (and holes through the consumption of hydrogen ions) is also encountered. This leads to the formation of hydrocarbon species, which are detected in a few studies when using methanol.[78,79]

From Fig. 1 we can progress in the utilization of adequate engineering efficiency factor(s) with the claimed dual aim of enclosing information concerning energy but also sustainability. In particular, we would discuss the consequences of using the selectivity factor and the potential of the "fraction of useful photons" factor, η_Θ. For each molecule of hydrogen generated,

Table 5 Summary of efficiency values presented in the literature for hydrogen production using ethanol as a sacrificial agent[61,85–92]

Catalyst	Source and radiation	Reaction conditions reagent/catalyst concentration	QE, PY, AQY, STH, PTEF/%	Ref.
1 wt% Pt/TiO_2	Black light blue (BLB) lamp 15 W 340–410 nm	Ethanol:H_2O 1:50 0.50 g L^{-1}	4.6	87
0.5 wt% Pt/TiO_2	Xe-lamp (300 or 450 W) Solar light-simulating light source	Ethanol:H_2O 0.04:1 1.3 g L^{-1}	50.0	88
0.25 wt% Pd/TiO_2	15 W BLB UV-lamp 15 W fluorescent visible light lamp UV-Vis	Ethanol:H_2O 1:50 0.15 g L^{-1}	UV: 34.8 UV-Vis: 8.8	85
0.25 wt% Pd/TiO_2	BLB near-UV lamp 15 W fluorescent visible light lamp UV-Vis	Ethanol:H_2O 1:50 0.15 g L^{-1}	13.7	86
0.25 wt% Pd/ TiO_2	BLB near-UV lamp 15 W fluorescent visible light lamp UV-Vis	Ethanol:H_2O 1:50 0.15 g L^{-1}	13.7	89
2 wt% Au/TiO_2	UV visible light (176 W) 0.24 mW cm^{-2} 254 nm	Ethanol:H_2O 1:3 1.3 g L^{-1} Opt.	61.2	90
1wt%Pt/(Nb)TiO_2	Hg-Xe lamp (500 W) 280–400 nm 420–680 nm	Ethanol:H_2O 3:7 0.50 g L^{-1} Opt.	UV: 4.0 Vis.: 1.0	61
1 wt% $Au/NaYF_4(Er^{3+}, Yb^{3+})$–CdS	Xe lamp (300 W) NIR (>700 nm)	Ethanol:H_2O 0.12:0.88 1.5 g L^{-1}	$9x10^{-4}$	91
7.4 wt% Ni/g-C_3N_4	20W fluorescent lamps Simulated sunlight	Ethanol:H_2O 1:9	1.7	92

Table 6 Summary of selectivity values presented in the literature for hydrogen production using ethanol as a sacrificial agent[61,84–86,92,93]

Catalyst	Source and radiation	Reaction conditions reagent/catalyst concentration	Product	Selectivity C basis/%	Selectivity H basis/%	Ref.
1 wt% Pt/TiO_2 1 wt% $Pt/(Nb)TiO_2$	Hg–Xe lamp (500 W) 280–400nm 420–680 nm	Ethanol:H_2O 3:7 0.50 g L^{-1} Opt.	Pt/TiO_2 UV H_2 CH_3CHO $CH_3CH_2COOCH_3$ Vis H_2 CH_3CHO $CH_3CH_2COOCH_3$ $Pt/(Nb)TiO_2$ UV H_2 CH_3CHO $CH_3CH_2COOCH_3$ Vis H_2 CH_3CHO $CH_3CH_2COOCH_3$	 — 81 19 — 71 29 — 89 11 — 97 3	 29.6 47.9 22.5 27.9 39.7 32.4 31.0 55.3 13.7 32.7 63.4 3.9	61
1 wt% Pt/TiO_2	Xe lamp (300 W)	Ethanol:H_2O 3:7 5 g L^{-1}	H_2 CH_3CHO $CH_3CHOHCHOHCH_3$	— 96.6 3.4	50.0 40.3 9.7	84
3.8 wt%Pt/3 wt% rGO-TiO_2	Hg lamp (450 W)	Ethanol:H_2O 2:8 0.50 g L^{-1}	H_2 CO_2	— 100	100 —	93
0.25 wt% Pd/TiO_2	BLB near-UV lamp 15 W fluorescent visible light lamp UV-Vis	Ethanol:H_2O 1:3 0.15 g L^{-1}	H_2 CH_3CHO CO CO_2 CH_4 CH_3CH_3 CH_2CH_2	— 34.8 7.0 0.9 1.7 10.4 45.2	12.5 31.2 — — 1.6 14.1 40.6	86
0.25 wt% Pd/TiO_2	15 W BLB UV-lamp 15 W fluorescent visible light lamp UV-Vis	Ethanol:H_2O 1:50 0.15 g L^{-1}	H_2 CH_3CHO CH_4 CH_3CH_3 CH_2CH_2	— 1.8 35.5 10.6 52.1	14.4 28.8 1.4 13.0 42.4	85
7.4 wt% Ni/g-C_3N_4	20W fluorescent lamps simulated sunlight	Ethanol:H_2O 1:9	H_2 CH_3CHO	— 100	31.3 68.7	92

essentially all steps of Fig. 1 would use two hole-type radicals. Thus for a pure photocatalytic, radical-triggered mechanism, whatever the selectivity, the S factor takes a value of 1/2 in the denominator of the efficiency, or in other words, the mentioned factor 2 multiplying the reaction rate in the numerator. This is true as far as thermal contributions to decarbonylation steps do not affect significantly the production of hydrogen. $\eta_\Theta(H_2)$ has always a constant factor of 2 differing from the quantum efficiency. A different question is the calculation of $\eta_\Theta(H)$. If "electron-consuming" products like hydrocarbons are generated in the process, the (weighted) sum of the hydrogen and methane reaction rates should be considered in the calculation, and, critically important, the selectivity factor per H atom is different for these two products (Fig. 1). Of course, all hydrogen containing products should be included in the calculation of $\eta_\Theta(H)$ but carbon-containing molecules presented in Fig. 1 and generated using hole-type species have a trivial treatment of the selectivity factor, as discussed above. Therefore, due to the inherent properties of the η_Θ parameter, the ratio of $\eta_\Theta(H_2)$ *vs.* $\eta_\Theta(H)$ expresses the atom-efficiency for the generation of hydrogen (ions) in terms of the "fraction" of photons consumed in the generation of the hydrogen molecule *vs.* the total photons used in the process that consumes the "generation" of H atoms. The η_Θ parameter can thus braid energy and sustainability information.

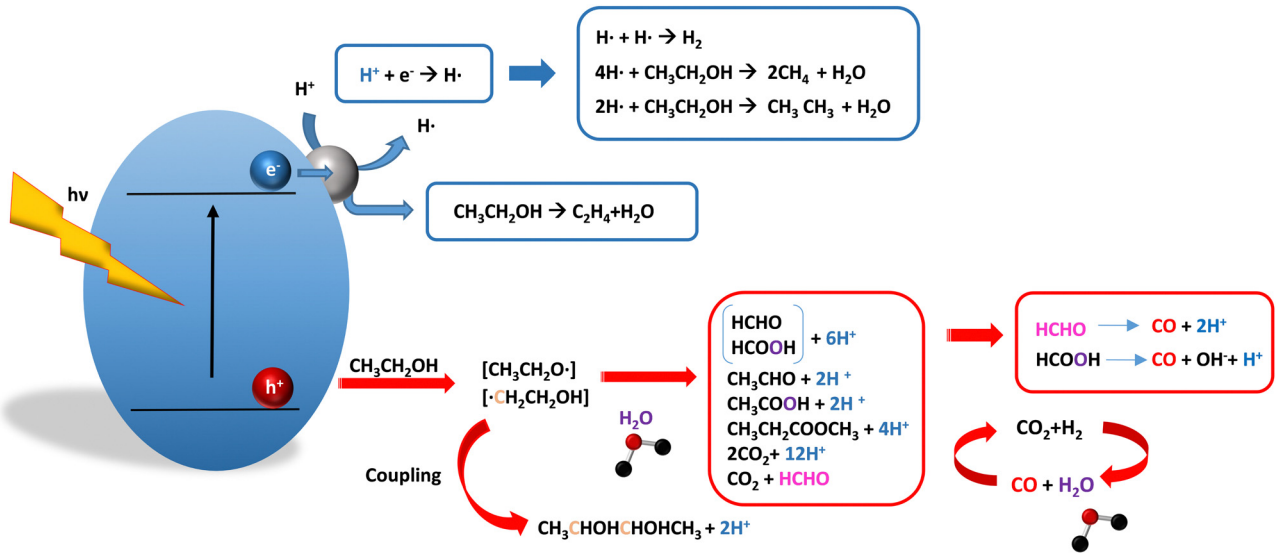

Fig. 2 Schematic representation of the radical species and intermediates detected in the photocatalytic production using ethanol as a sacrificial molecule. Colour codes are explained in the text.

Table 7 Summary of efficiency values presented in the literature for hydrogen production using glycerol as a sacrificial agent[98–103]

Catalyst	Source and radiation	Reaction conditions reagent/catalyst concentration	QE, PY, AQY, STH, PTEF/%	Ref.
1 wt% Pt/TiO_2	8 W black lamps Max. 365 nm	$C_3H_8O_3$:H_2O 0.03:1	10.2	98
1 wt% Pt/TiO_2	Hg lamp (1000 W) 313–366 nm	$C_3H_8O_3$:H_2O 0.03:1 0.67 g L^{-1}	0.08	99
1 wt% Pt/N-TiO_2 (nanotubes)	Fluo (Philips HPL-N 250 W/542 E40 HG 1SL) 17% UV + 83% Vis	$C_3H_8O_3$:H_2O 1:9 1 g L^{-1}	37.4	100
2.8 wt% Ag_2O /TiO_2	Xe lamp (300 W) 320–780 nm	$C_3H_8O_3$:H_2O 0.07:1 2 g L^{-1}	10.9	101
2.5 wt% CuO_x/TiO_2	Hg lamp (125 W)	$C_3H_8O_3$:H_2O 0.07:1 0.50 g L^{-1}	29.0	102
1:10 w/w CuO–TiO_2	Sunlight compound parabolic collector	$C_3H_8O_3$:H_2O 0.005:1 2.1 g L^{-1} Opt.	1,4	103

This $\eta_\Theta(H_2)$ observable is the most informative factor describing the (energy-related) efficiency of the reaction as it measures the faction of initial photons used to generate hydrogen and can be used straightforwardly in the calculation of the global efficiency of the process. Besides that, the above mentioned $\eta_\Theta(H_2)$ *vs.* $\eta_\Theta(H)$ ratio allows the inclusion of sustainability related to the atom-efficiency in the use of hydrogen atoms by the photocatalytic system. We again recall that depending on the reaction products encountered (Table 3 and Fig. 1), the hydrogen atoms come from the sacrificial molecules exclusively or also from water.

As discussed in the introduction, a parallel point is the selective formation of specific carbon-containing intermediates. This fact can contribute to making the process "fully" sustainable. Examples of catalysts having high selectivity on a carbon basis are presented in Table 3. Of course, we can delineate the $\eta_\Theta(C_p)$ *vs.* $\eta_\Theta(C)$ ratio to analyze the carbon-based selectivity of the reaction on a photon basis. In this ratio, $\eta_\Theta(C_p)$ is the fraction of useful photons utilized to obtain the desired (carbon-containing) products. From Fig. 1 and the procedures outlined above, we can calculate easily the selectivity factors for the $\eta_\Theta(C_p)$ and $\eta_\Theta(C)$ parameters. A simple

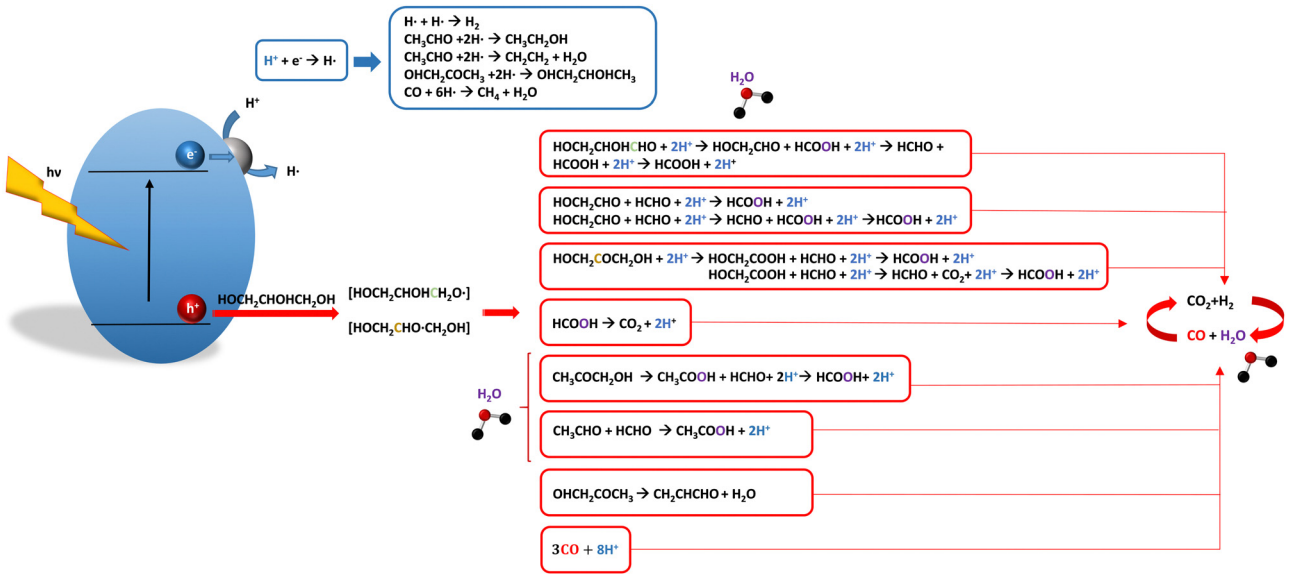

Fig. 3 Schematic representation of the radical species and intermediates detected in the photocatalytic production using glycerol as a sacrificial molecule. Colour codes are explained in the text.

Table 8 Summary of selectivity values presented in the literature for hydrogen production using glycerol as a sacrificial agent

Catalyst	Source and radiation	Reaction conditions reagent/ catalyst concentration	Product	Selectivity C basis/%	Selectivity H basis/%	Ref.
1 wt% Rh/TiO_2	300 W Xe lamp	$C_3H_8O_3:H_2O$ 0.75 g L^{-1}	H_2	—	70.8	96
			$C_2H_4O_2$	61.2	29.2	
			CO_2	38.8	—	
0.1 wt% Ag–0.3 wt% Pd/TiO_2	100 W UV lamp ≥360 nm	$C_3H_8O_3:H_2O$ 1:20 0.25 g L^{-1}	H_2	—	2.2	97
			CO	0.08	—	
			CO_2	2.4	—	
			HCHO	21.0	20.3	
			$C_2H_6O_2$	7.4	10.7	
			$C_3H_6O_2$	69.1	66.8	

inspection of the figure shows that the calculation of the selectivity factor corresponding to $\eta_\Theta(C_p)$ is not as simple as the case of $\eta_\Theta(H_2)$, that is, is not a constant.

3.3. Ethanol

As it is obvious, in the case of ethanol, more intermediates could be formed but several potentially feasible paths are not supported by experimental evidence. In any case, Table 5 summarizes efficiency values for the production of hydrogen using this molecule. The results concerning efficiency parameters allowing quantitative measurement mainly concern titania-based systems, promoted with different noble metals and/or doping. A few non-titania systems are collected at the end of the table. From the inspection of Table 5, it is also plausible that the true efficiency, as measured by the quantum efficiency, can reach a value of around 10% using this molecule. The results concern the use of the UV-visible region although up to *ca.* 600 nm, but not the whole UV-visible-nearIR range of the solar spectrum. Considering the evolution of the sacrificial molecule, Table 6 collects the reports with careful investigation of the selectivity and Fig. 2 summarizes the results. We encountered relatively similar results to the more explored case of methanol. As can be seen in Fig. 2, the hole-triggered radicals detected are two. One oxygen-centered alkoxy-type radical and one carbon-centered radical corresponding to the CH_3 moiety of the alcohol molecule. Other possible radicals are rather unlikely and unstable. Similarly to the methanol case, the alkoxy radical leads to the chain-type mechanism generating acetaldehyde, acetic acid and carbon dioxide. Decarbonylation reactions, the subsequent water gas shift equilibrium reaction, as well as "coupling" intermediates such as ethyl acetate can be also generated through this path. In addition, C_1 products generated from the rupture of the C–C bond are sometimes observed.[61,83] From the carbon-centered radical, we are only aware of the selective generation (96.6% selectivity on a carbon basis) of 2,3-butanediol (Table 5 and Fig. 2).[84] In the case of ethanol, the presence of hydrocarbons was again detected, but a higher number of such molecules can be formed (Fig. 2).[85,86] With the reaction scheme being rather parallel to the ethanol case, except for the C–C breaking products, the analysis described above essentially holds for the ethanol case. Thus, the mentioned possible achievement of

Table 9 Summary of efficiency values presented in the literature for hydrogen production using biomass as a sacrificial agent[61,76,88,104,105,107–119]

Catalyst	Source and Radiation	Reaction conditions reagent/catalyst concentration	QE, PY, AQY, STH, PTEF/%	Ref.
1.5 wt% P, 3 wt% Ni-doped TiO_2	Two solar simulator bulbs (300 W) >420 nm	Ethylene glycol:H_2O 1:10 1 g L^{-1}	34.9	107
1 wt% Pt/(Nb)TiO_2	Hg–Xe lamp (500 W) 280–400 nm 420–680 nm	2-Propanol:H_2O 1:10 0.50 g L^{-1} Opt.	UV: 1.8 Vis: 0.8	61
5 wt% Pt CdS	Xe lamp (1000 W) 430–520 nm	Lactic acid:H_2O 1:10 6 g L^{-1}	0.71	105
0.8 wt% NiB/CdS	Xe lamp (300 W) 420 nm	Lactic acid:H_2O 1:10 0.66 g L^{-1}	21	108
0.79 wt% NiS/CdS	Xenon lamp (300 W) >420 nm	Lactic acid:H_2O 30:70 3 g L^{-1}	51.3	109
0.2 wt% MoS_2/CdS	Xe lamp (300 W) >420 nm	Lactic acid:H_2O 10:90 0.50 g L^{-1}	7.3	110
20 wt% NiS/CdS	300 W Xe lamp λ >400 nm	Lactic acid Lactic and lignin acid 1 g L^{-1}	29.3 44.9	111
GaN:ZnO	Xe lamp (300 W) λ >420 nm	Ascorbic acid (10 mM) 0.25 g L^{-1}	5.1	76
Zn-tri-PcNc-g-C_3N_4	300 W Xe lamp ≥ 500 nm	H_2O Ascorbic acid (8.8 g L^{-1}) 1 g L^{-1} Opt	1.85	112
0.5 wt% Pt/Zn-tri-PcNc-2/g-C_3N_4	300 W Xe lamp 700 nm	H_2O Ascorbic acid (8.8 g L^{-1}) 1 g L^{-1}	1.07	113
ZnPyd/C_3N_4	300 W Xe lamp ≥420 nm	H_2O Ascorbic acid (8.8 g L^{-1}) 1.5 g L^{-1}	32.3	114
1.5 wt% Pt/ZnMT3PyP/g-C_3N_4	300 W Xe lamp ≥420 nm	H_2O Ascorbic acid (8.8 g L^{-1}) 1.5 g L^{-1}	25.1	115
0.5 wt% Pt/TiO_2	Xe-arc lamp (450 W) 365 nm	Glucose:H_2O 7:60 1,33 g L^{-1}	63	88
0.1 wt% Ru/$ZnIn_2S_4$	LED irradiation (9.6 W) 455 nm	CH_3CN:2,5-DMF 1:1 10 g L^{-1}	15.2	104
0.3 wt% Pt/TiO_2	4 × UV-A lamp (15 W) 366 nm	Swine sewage:H_2O 1.7:100 2 g L^{-1} Opt.	0.0052	116
1.0 wt% Pt/TiO_2	300 W Xe lamp 380 nm	Alpha cellulose:H_2O 3.1:1000 0.40 g L^{-1}	1.84	117
2 wt% TiO_2/MoS_2	300 W Xe lamp 380 nm	Alpha cellulose:H_2O 3.1:1000 0.40 g L^{-1}	1.45	118
0.5 wt% Pt NCs/TiO_2	300 W Xe lamp 380 nm	Lignocellulose:H_2O 0.18:1000 0.25 g L^{-1}	4.1	119

a 10% profit of sunlight appears feasible and supported by the results of Table 5, although with the associated challenges just outlined for the methanol case. On the other hand, the generation of a significant number of products challenges the

Table 10 Summary of selectivity values presented in the literature for hydrogen production using biomass as a sacrificial agent

Catalyst	Source and radiation	Reaction conditions reagent/ catalyst concentration	Product	Selectivity C basis/%	Selectivity H basis/%	Ref.
0.1 wt% Ru/$ZnIn_2S_4$	LED irradiation (9.6 W) 455 nm	CH_3CN : 2,5-DMF 1 : 1 10 g L^{-1}	H_2	—	63.3	104
			Dimers (C12)	68.3	17.8	
			Trimers (C18)	28.3	4.0	
			Tetramers (C24)	3.3	14.8	
5 wt% Pt/CdS	1000 W Xe lamp 430–520 nm	Lactic acid : H_2O 1 : 10 6 g L^{-1}	H_2	—	45.1	105
			CO_2	2.1	—	
			$CH_3COCOOH$	97.9	54.9	

obtaining of high selectivity on a carbon basis, although Table 6 includes some cases. It is also evident that both the frequent presence of hydrocarbons as products and the relatively low selectivity to carbon dioxide (or, in other words, the higher number of products) observed in the majority of cases would lead to lower values of the $\eta_\Theta(H_2)$ *vs.* $\eta_\Theta(H)$ ratio. Thus, the sustainability of ethanol as a sacrificial molecule for hydrogen generation would not reach values as in the case of methanol.

3.4. Glycerol

For glycerol, data concerning efficiency values are presented in Table 7. Although the results are encouraging, a complete lack of reports containing information extracted from the quantum efficiency parameter can be noticed. The STH parameter could render a value near 1% under sunlight excitation. This indicates that glycerol would be a far more thought molecule to obtain a significant profit from sunlight. There are several studies analyzing qualitatively (*e.g.* detection of products) the evolution of the glycerol molecule in the reaction. These studies used titania-based materials and are summarized in Fig. 3, where we can see that only oxygen-centered radicals are considered for the formation of intermediates. The formation of electron-consuming products, competing with hydrogen, was also reported.[94–96] As shown in Table 8, only a couple of contributions reported the full analysis of the selectivity,[96,97] and thus there is limited information in this case to progress in the quantitative analysis of energy and sustainability issues.

3.5. Other sacrificial molecules

We can briefly discuss the case of carbon-containing molecules using other (than those previously studied here) biomass-derived molecules which may strengthen the sustainability of the process. Table 9 summarizes the results considering other alcohols such as ethylene glycol and 2-propanol, acids such as lactic acid and ascorbic acid, sugars such as glucose, as well as more complex substrates such as 2,5-dimethylfuran, alpha-cellulose and lignocellulose. Catalysts utilized are oxides, nitrides, sulfides, MOFs, or carbon nitride sensitized with dyes, porphyrins or phthalocyanines. Similarly to the glycerol case, there is limited information although a couple of results using the photonic yield parameter suggest that glucose can be an ideal choice for generating hydrogen. The selectivity of the reaction is scarcely studied. Table 10 summarizes a couple of results encountered where the production of diesel precursors from 2,5-DMF[104] or of pyruvic acid from lactic acid[105] is achieved with high (carbon basis) selectivity and with the concomitant production of hydrogen. It can be also mentioned that hydrogen generation from biomolecules, for example ethanol, can be used in a cascade-type process to trigger hydrogenation steps of other biomolecules to render valuable products, such as benzimidazole derivatives.[106]

Finally, for completeness, we collected selected results for efficiency calculations using other sacrificial molecules of use in the field such as TEOA. The results are compiled in Table 11. The catalysts employed with this sacrificial agent included the frequently utilized molecular-type catalysts such as carbon nitride but also composite systems with dyes such as erythrosine B and eosin Y, as well as porphyrins or phthalocyanines. High values of efficiency can be observed in several cases but using parameters having a limited utility, as earlier discussed in this work using methanol, where a most complete database is available. Thus, their potential to achieve the 10% profit from solar light is still to be ascertained.

4. Conclusions

Nowadays, the photocatalytic generation of hydrogen attempts to produce this energy vector using renewable energy sources and reactants. To reach a holistic approach towards the settlement of a clean, green hydrogen production and explore the future of the process, the setting up of parameters allowing a quantitative measurement of both the energetic and sustainability implications of the process appears as a must.

To this end, here we surveyed the literature available parameters primarily oriented to measuring efficiency. Efficiency parameters are defined by the IUPAC for photocatalytic processes, with quantum efficiency being the one that allows a rigorous metrics to evaluate the global efficiency of a process. From this, we delineated the work aiming to progress further in the evaluation of both energetic and sustainability sides of the hydrogen photocatalytic process using a quantum efficiency related parameter, the so-called ''fraction of useful photons''. This parameter allows the true calculation of the global efficiency, rendering a dimensionless parameter, but also expresses the hydrogen atom efficiency of hydrogen production in a photon-based metrics. In addition, up to four additional parameters, all of them demanding less experimental–computational effort in their calculation, were considered. These go from the photonic yield parameter defined by the IUPAC, to

Table 11 Summary of efficiency values presented in the literature for hydrogen production using several sacrificial molecules as a sacrificial agent[120–136]

Catalyst	Source and radiation	Reaction conditions reagent/catalyst concentration	QE, PY, APY, STH, PTEF/%	Ref.
CdS	300 W Xe lamp 430 nm	Na_2S 1.6 g L^{-1} Na_2SO_3 6.3 g L^{-1} 0.56 g L^{-1} Opt.	0.47	120
$Cd_{0.5}Zn_{0.5}S$	300 W Xe lamp 300–760 nm	Na_2S (0.35M) Na_2SO_3 (0.25 M) 0.56 g L^{-1}	43.0	121
0.9 wt% Pt/33 mol% CdS–TiO_2	Solar light-simulating source (Osram XBO 450 W) 470 nm	Na_2S/Na_2SO_3 and ethanol 1.3 g L^{-1}	20.0	122
0.3 wt% Pt–0.13 wt% PdS/CdS	300 W Xe lamp >420 nm	Na_2S (0.5 M) and Na_2SO_3 (0.5 M) 1.5 g L^{-1}	93.0	123
7.5 wt% single-atom Ni/TiO_2-g-C_3N_4	300 W Xe lamp 420 nm, 500 nm, 550 nm	TEOA:H_2O 1:9 0.33 g L^{-1}	15.0	124
$CdLa_2S_4$/15 wt% Ni_2P	300 W Xe lamp >420 nm	TEOA:H_2O 1:9 0.90 g L^{-1}	1.4	125
S-Doped g-C_3N_4	300 W Xe lamp >420 nm	TEOA:H_2O 1:9 0.50 g L^{-1}	13.7	126
g-C_3N_4	300 W Xe lamp >420 nm	TEOA:H_2O 1:9 g L^{-1}	10.9	127
g-C_3N_4	300 W Xe lamp 400 nm	TEOA:H_2O 1:9 0.50 g L^{-1}	13.5	128
1 wt% Pt/N-defective g-C_3N_4	300 W Hg lamp 420 nm	TEOA:H_2O 7:93 0.3 g L^{-1}	27.1	129
1 wt% Pt/g-C_3N_4/PHI	300 W Hg lamp 420, 450,475, 500 nm	TEOA:H_2O 1:9 1 g L^{-1}	1.7, 1.5, 0.8, 0.4	130
MgPc/3%Pt/g-C_3N_4	300 W Xe lamp 420 nm	TEOA:H_2O 1:10 1 g L^{-1}	5.6	131
EY-g-C_3N_4-7%Pt	300 W Hg lamp ≥420 nm	TEOA:H_2O 1.25 g L^{-1}	18.8	132
N-Annulated perylene-g-C_3N_4	300 W Xe lamp 520 nm	TEOA:H_2O 1:5 0.83	27.32	133
EB-MoS_x-g-C_3N_4	400 W Hg lamp ≥420 nm	TEOA:H_2O 1.25 g L^{-1}	8.3	134
ZnPc-1.5%Pt/K^+-g-C_3N_4	300 W Xe lamp ≥ 420 nm	TEOA:H_2O 1:9 1.5 g L^{-1}	2.74	135
P-CTFs	300 W Xe lamp ≥420 nm	TEOA:H_2O 1:10 0.4 g L^{-1}	4.65	136

other broadly used parameters such as the solar-to-hydrogen efficiency. These parameters focus on the energetic side of the problem but, unfortunately, would not inform straightforwardly about the possible energy-related losses and the ways to circumvent them. In spite of it, their simplicity compared with the quantum efficiency related parameters makes their use broad and appealing. The article also described briefly the application of new tools based on artificial intelligence in the field. We stressed the point that the results would indicate that the knowledge of the rate of photon absorption or simpler yet related parameters appears unavoidable to obtain useful information.

We utilized the set of six parameters (quantum efficiency, fraction of useful photons, photonic yield, apparent (photonic) yield, solar-to-hydrogen and photochemical thermodynamic efficiency factor) to evaluate the field of photocatalytic production of hydrogen. In parallel, the perspective article paid particular attention to the interpretation of the physical basis

of the quantum efficiency and the fraction of useful photon parameters. We sorted out the research published in the field considering the different catalytic processes studied. Starting with the use of water in the splitting reaction, we analyzed the use of different sacrificial molecules, paying particular attention to the use of renewable sacrificial molecules, particularly alcohols which can come from fermentation and other bio-based processes.

With water being a potentially optimal reactant, the results of the literature considering the whole use of the solar spectrum would indicate that research output is far from achieving the benchmark value of 10%. For sacrificial molecules, analysis of the dual-aim "fraction of useful photons" parameter was carried out in terms of both the charge-carrier utilization and the molecules' (and water) roles and evolution under reaction conditions, and the result utilized to interpret the capability of any catalytic system in terms of energy and sustainability and thus to serve as a firm ground to guide the future of the field. The survey of the sacrificial molecules studied in the literature would indicate that methanol and (to a somewhat lower extent) ethanol can be optimal choices. Glucose could be also a good choice in terms of energy related issues. For the cases of methanol and ethanol, it appears that titania-based composite systems are close to the 10% cuff-off value in the UV-visible range, but the efficient use of the complete solar spectrum is still challenging. In particular, the nearIR region would need to be fruitfully utilized. According to the literature results, this would require a more intensive exploration of multicomponent composite systems, where, in addition to the co-catalyst presence, the (titania) oxide based systems would be doped and/or accompanied with lanthanide and/or carbon elements (doping) and semiconductors (composite). A more exhaustive analysis of other alternatives, such as the two photon technologies, awaits in the future in order to show potential in the field.

The analysis has been extended to other sacrificial molecules of interest, such as glycerol coming from the transesterification of fatty acids (triglycerides) and other processes, or less commonly tested molecules such as isopropanol, lignin acid, and others. Unfortunately, the limited and (relatively) low quality of the information precludes any rigorous analysis, although in most cases, the benchmark value of 10% of the solar spectrum light appears unattainable with current capabilities.

Acronyms

APY	Apparent photonic yield
2,5-DMF	2,5-Dimethylfuran
COFs	Covalent organic frameworks
C12 dimers	$C_{12}H_{18}O_2$
	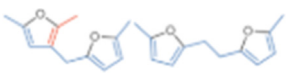
EB	Erythrosin B
EY	Eosin Y
MgPc	Magnesium phthalocyanine
Opt.	Mass of the catalysts optimized
P25	TiO_2 (Evonik ©)
PcNc	Phthalocyanine
P-CTFs	Phosphorus-doped covalent triazine-based frameworks
PHI	Poly(heptazine imide)
PTFE	Photochemical thermodynamic efficiency factor
Pt NCs	Platinum nanoclusters
PY	Photonic yield
QE	Quantum efficiency
STH	Solar to hydrogen
STOS	$Sm_2Ti_2O_5S_2$
TEOA	Triethanolamine
Tetramers	$C_{24}H_{26}O_4$
C18 trimers	$C_{18}H_{20}O_3$
	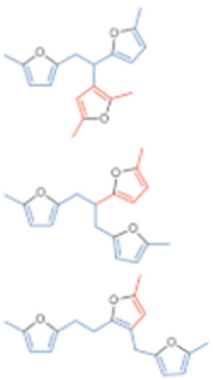
$ZnMT_3PyP$	Zinc-5-(4-carboxyphenyl)-10,15,20-tri(3-pyridyl)porphyrin
ZnPc	Zinc phthalocyanine
ZnPyd	Zn-metalloporphyrins

Data availability

Data will be available upon request to the authors.

Conflicts of interest

The authors declare no conflict of interest.

Acknowledgements

The authors acknowledge the financial support through grant and PID2022-136883OB-C21. The project is funded by MCIN/AEI/10.13039/501100011033 (Spain). M. F. G. is deeply indebted to Prof. F. Fernández-Martín for multiple discussions.

References

1 J. Zhao, R. Shi, Z. Li, C. Zhou and T. Zhang, *Nano Sel.*, 2020, **1**, 12–29.
2 U. Mondal and G. D. Yadav, *Green Chem.*, 2021, **23**, 8361–8405.
3 X. Chen, S. Shen, L. Guo and S. S. Mao, *Chem. Rev.*, 2010, **110**, 6503–6570.

4 A. Kubacka, M. Fernández-García and G. Colón, *Chem. Rev.*, 2012, **112**, 1555–1614.
5 D. Rodríguez-Padrón, R. Luque and M. J. Muñoz-Batista, *Top. Curr. Chem.*, 2020, **378**, 1–28.
6 S. Alsayegh, J. R. Johnson, B. Ohs, J. Lohaus and M. Wessling, *Int. J. Hydrogen Energy*, 2017, **42**, 6000–6011.
7 H. Idriss, *Energy Technol.*, 2021, **9**, 2000843.
8 V. Kumaravel, M. Imam, A. Badreldin, R. Chava, J. Do, M. Kang and A. Abdel-Wahab, *Catalysts*, 2019, **9**, 276.
9 M. Ismael, *Sol. Energy*, 2020, **211**, 522–546.
10 H. H. Do, D. L. T. Nguyen, X. C. Nguyen, T.-H. Le, T. P. Nguyen, Q. T. Trinh, S. H. Ahn, D.-V. N. Vo, S. Y. Kim and Q. Van Le, *Arabian J. Chem.*, 2020, **13**, 3653–3671.
11 R. Liu, H. Yin, P. Guo, X. Liu and Z. Yin, *Energy Technol.*, 2024, 2301708.
12 O. M. Alfano, D. Bahnemann, A. E. Cassano, R. Dillert and R. Goslich, *Catal. Today*, 2000, **58**, 199–230.
13 U. Caudillo-Flores, M. J. Muñoz-Batista, M. Fernández-García and A. Kubacka, *Catal. Rev.*, 2024, **66**, 531–585.
14 M. Qureshi and K. Takanabe, *Chem. Mater.*, 2017, **29**, 158–167.
15 A. Kubacka, I. Barba-Nieto, U. Caudillo-Flores and M. Fernández-García, *Curr. Opin. Chem. Eng.*, 2021, **33**, 100712.
16 S. E. Braslavsky, A. M. Braun, A. E. Cassano, A. V. Emeline, M. I. Litter, L. Palmisano, V. N. Parmon and N. Serpone, *Pure Appl. Chem.*, 2011, **83**, 931–1014.
17 M. Melchionna and P. Fornasiero, *ACS Catal.*, 2020, **10**, 5493–5501.
18 Z. Chen, T. F. Jaramillo, T. G. Deutsch, A. Kleiman-Shwarsctein, A. J. Forman, N. Gaillard, R. Garland, K. Takanabe, C. Heske, M. Sunkara, E. W. McFarland, K. Domen, E. L. Miller, J. A. Turner and H. N. Dinh, *J. Mater. Res.*, 2010, **25**, 3–16.
19 T. Hisatomi and K. Domen, *Nat. Catal.*, 2019, **2**, 387–399.
20 S. Cao and L. Piao, *Angew. Chem., Int. Ed.*, 2020, **59**, 18312–18320.
21 L. Sun and J. R. Bolton, *J. Phys. Chem.*, 1996, **100**, 4127–4134.
22 H. de Lasa, B. S. Rosales, J. Moreira and P. Valades-Pelayo, *Chem. Eng. Technol.*, 2016, **39**, 51–65.
23 F. Machuca-Martínez, M. A. Mueses, J. Colina-Márquez and G. L. Puma, Photocatalytic Reactor Modeling, *RSC*, 2016, ch. 16, pp. 388–424.
24 Y. Boyjoo, H. Sun, J. Liu, V. K. Pareek and S. Wang, *Chem. Eng. J.*, 2017, **310**, 537–559.
25 L. Zhang and W. A. Anderson, *Chem. Eng. Sci.*, 2010, **65**, 1513–1521.
26 J. E. Duran, F. Taghipour and M. Mohseni, *J. Photochem. Photobiol., A*, 2010, **215**, 81–89.
27 Y. Boyjoo, M. Ang and V. Pareek, *Chem. Eng. Sci.*, 2014, **111**, 34–40.
28 J. Moreno, C. Casado and J. Marugán, *Chem. Eng. Sci.*, 2019, **205**, 151–164.
29 O. M. Alfano, A. E. Cassano, J. Marugán and R. van Grieken, Fundamentals of Radiation Transport in Absorbing Scattering Media, *RSC*, 2016, ch. 14, pp. 349–366.
30 Y. Haghshenas, W. P. Wong, D. Gunawan, A. Khataee, R. Keyikoğlu, A. Razmjou, P. V. Kumar, C. Y. Toe, H. Masood, R. Amal, V. Sethu and W. Y. Teoh, *EES Catal.*, 2024, **2**, 612–623.
31 A. Kubacka, U. Caudillo-Flores, I. Barba-Nieto and M. Fernández-García, *Appl. Catal., A*, 2021, **610**, 117966.
32 B. A. Pinaud, J. D. Benck, L. C. Seitz, A. J. Forman, Z. Chen, T. G. Deutsch, B. D. James, K. N. Baum, G. N. Baum, S. Ardo, H. Wang, E. Miller and T. F. Jaramillo, *Energy Environ. Sci.*, 2013, **6**, 1983.
33 A. Gupta, B. Likozar, R. Jana, W. C. Chanu and M. K. Singh, *Int. J. Hydrogen Energy*, 2022, **47**, 33282–33307.
34 Y. Yang, X. Chu, H.-Y. Zhang, R. Zhang, Y.-H. Liu, F.-M. Zhang, M. Lu, Z.-D. Yang and Y.-Q. Lan, *Nat. Commun.*, 2023, **14**, 593.
35 H. Nishiyama, T. Yamada, M. Nakabayashi, Y. Maehara, M. Yamaguchi, Y. Kuromiya, Y. Nagatsuma, H. Tokudome, S. Akiyama, T. Watanabe, R. Narushima, S. Okunaka, N. Shibata, T. Takata, T. Hisatomi and K. Domen, *Nature*, 2021, **598**, 304–307.
36 H. Kato, Y. Sasaki, N. Shirakura and A. Kudo, *J. Mater. Chem. A*, 2013, **1**, 12327.
37 Q. Wang, T. Hisatomi, Q. Jia, H. Tokudome, M. Zhong, C. Wang, Z. Pan, T. Takata, M. Nakabayashi, N. Shibata, Y. Li, I. D. Sharp, A. Kudo, T. Yamada and K. Domen, *Nat. Mater.*, 2016, **15**, 611–615.
38 Q. Wang, T. Hisatomi, Y. Suzuki, Z. Pan, J. Seo, M. Katayama, T. Minegishi, H. Nishiyama, T. Takata, K. Seki, A. Kudo, T. Yamada and K. Domen, *J. Am. Chem. Soc.*, 2017, **139**, 1675–1683.
39 K. Sayama, K. Mukasa, R. Abe, Y. Abe and H. Arakawa, *Chem. Commun.*, 2001, 2416–2417.
40 J. Kim, D. W. Hwang, H. G. Kim, S. W. Bae, J. S. Lee, W. Li and S. H. Oh, *Top. Catal.*, 2005, **35**, 295–303.
41 S. Sun, T. Hisatomi, Q. Wang, S. Chen, G. Ma, J. Liu, S. Nandy, T. Minegishi, M. Katayama and K. Domen, *ACS Catal.*, 2018, **8**, 1690–1696.
42 R. Abe, T. Takata, H. Sugihara and K. Domen, *Chem. Commun.*, 2005, 3829.
43 K. Maeda, M. Higashi, D. Lu, R. Abe and K. Domen, *J. Am. Chem. Soc.*, 2010, **132**, 5858–5868.
44 X. Chen, R. Shi, Q. Chen, Z. Zhang, W. Jiang, Y. Zhu and T. Zhang, *Nano Energy*, 2019, **59**, 644–650.
45 H. Su, W. Che, F. Tang, W. Cheng, X. Zhao, H. Zhang and Q. Liu, *J. Phys. Chem. C*, 2018, **122**, 21108–21114.
46 Y. Goto, T. Hisatomi, Q. Wang, T. Higashi, K. Ishikiriyama, T. Maeda, Y. Sakata, S. Okunaka, H. Tokudome, M. Katayama, S. Akiyama, H. Nishiyama, Y. Inoue, T. Takewaki, T. Setoyama, T. Minegishi, T. Takata, T. Yamada and K. Domen, *Joule*, 2018, **2**, 509–520.
47 T. Takata, J. Jiang, Y. Sakata, M. Nakabayashi, N. Shibata, V. Nandal, K. Seki, T. Hisatomi and K. Domen, *Nature*, 2020, **581**, 411–414.
48 H. Kato and A. Kudo, *J. Phys. Chem. B*, 2001, **105**, 4285–4292.
49 U. Caudillo-Flores, A. Kubacka, T. Berestok, T. Zhang, J. Llorca, J. Arbiol, A. Cabot and M. Fernández-García, *Int. J. Hydrogen Energy*, 2020, **45**, 1510–1520.

50 E. Pulido Melián, O. González Díaz, A. Ortega Méndez, C. R. López, M. Nereida Suárez, J. M. Doña Rodríguez, J. A. Navío, D. Fernández Hevia and J. Pérez Peña, *Int. J. Hydrogen Energy*, 2013, **38**, 2144–2155.
51 M. Edelmannová, M. de los Milagros Ballari, M. Přibyl and K. Kočí, *Energy Convers. Manage.*, 2021, **245**, 114582.
52 O. Fontelles-Carceller, M. J. Muñoz-Batista, E. Rodríguez-Castellón, J. C. Conesa, M. Fernández-García and A. Kubacka, *J. Catal.*, 2017, **347**, 157–169.
53 E. P. Melián, C. R. López, A. O. Méndez, O. G. Díaz, M. N. Suárez, J. M. D. Rodríguez, J. A. Navío and D. F. Hevia, *Int. J. Hydrogen Energy*, 2013, **38**, 11737–11748.
54 M. P. Languer, F. R. Scheffer, A. F. Feil, D. L. Baptista, P. Migowski, G. J. Machado, D. P. de Moraes, J. Dupont, S. R. Teixeira and D. E. Weibel, *Int. J. Hydrogen Energy*, 2013, **38**, 14440–14450.
55 A. Naldoni, M. D'Arienzo, M. Altomare, M. Marelli, R. Scotti, F. Morazzoni, E. Selli and V. Dal Santo, *Appl. Catal., B*, 2013, **130–131**, 239–248.
56 K. Ćwieka, Z. Bojarska, K. Czelej, D. Łomot, P. Dziegielewski, A. Maximenko, K. Nikiforow, L. Gradoń, M. Qi, Y. Xu and J. C. Colmenares, *Chem. Eng. J.*, 2023, **474**, 145687.
57 H. Wang, H. Qi, X. Sun, S. Jia, X. Li, T. J. Miao, L. Xiong, S. Wang, X. Zhang, X. Liu, A. Wang, T. Zhang, W. Huang and J. Tang, *Nat. Mater.*, 2023, **22**, 619–626.
58 J. A. Ortega Méndez, C. R. López, E. Pulido Melián, O. González Díaz, J. M. Doña Rodríguez, D. Fernández Hevia and M. Macías, *Appl. Catal., B*, 2014, **147**, 439–452.
59 E. Pulido Melián, M. Nereida Suárez, T. Jardiel, D. G. Calatayud, A. del Campo, J. M. Doña-Rodríguez, J. Araña and O. M. González Díaz, *Int. J. Hydrogen Energy*, 2019, **44**, 24653–24666.
60 I. Barba-Nieto, K. C. Christoforidis, M. Fernández-García and A. Kubacka, *Appl. Catal., B*, 2020, **277**, 119246.
61 O. Fontelles-Carceller, M. J. Muñoz-Batista, J. C. Conesa, A. Kubacka and M. Fernández-García, *Mol. Catal.*, 2018, **446**, 88–97.
62 O. Fontelles-Carceller, M. J. Muñoz-Batista, J. C. Conesa, M. Fernández-García and A. Kubacka, *Appl. Catal., B*, 2017, **216**, 133–145.
63 U. Caudillo-Flores, M. J. Muñoz-Batista, M. Fernández-García and A. Kubacka, *Appl. Catal., B*, 2018, **238**, 533–545.
64 L. A. Arce-Saldaña, U. Caudillo-Flores, R. Sayago-Carro, G. Soto-Herrera, M. Fernández-García and A. Kubacka, *Catal. Today*, 2023, **419**, 114148.
65 J. Yu, Y. Hai and B. Cheng, *J. Phys. Chem. C*, 2011, **115**, 4953–4958.
66 H. Wang, H. Jiang, P. Huo, M. Filip Edelmannová, L. Čapek and K. Kočí, *J. Environ. Chem. Eng.*, 2022, **10**, 106908.
67 L. Li, B. Cheng, Y. Wang and J. Yu, *J. Colloid Interface Sci.*, 2015, **449**, 115–121.
68 I. Barba-Nieto, G. Colón, M. Fernández-García and A. Kubacka, *Chem. Eng. J.*, 2022, **442**, 136333.
69 L. Lin, Y. Ma, J. J. M. Vequizo, M. Nakabayashi, C. Gu, X. Tao, H. Yoshida, Y. Pihosh, Y. Nishina, A. Yamakata, N. Shibata, T. Hisatomi, T. Takata and K. Domen, *Nat. Commun.*, 2024, **15**, 397.
70 S. Y. Toledo Camacho, A. Rey, M. D. Hernández-Alonso, J. Llorca, F. Medina and S. Contreras, *Appl. Surf. Sci.*, 2018, **455**, 570–580.
71 C.-W. Tsao, S. Narra, J.-C. Kao, Y.-C. Lin, C.-Y. Chen, Y.-C. Chin, Z.-J. Huang, W.-H. Huang, C.-C. Huang, C.-W. Luo, J.-P. Chou, S. Ogata, M. Sone, M. H. Huang, T.-F. M. Chang, Y.-C. Lo, Y.-G. Lin, E. W.-G. Diau and Y.-J. Hsu, *Nat. Commun.*, 2024, **15**, 413.
72 R. Jiang, L. Mao, Y. Zhao, J. Zhang, X. Cai and X. Gu, *J. Colloid Interface Sci.*, 2022, **606**, 317–327.
73 S. Xie, Z. Shen, J. Deng, P. Guo, Q. Zhang, H. Zhang, C. Ma, Z. Jiang, J. Cheng, D. Deng and Y. Wang, *Nat. Commun.*, 2018, **9**, 1181.
74 X. Zheng, Y. Song, Y. Liu, Y. Yang, D. Wu, Y. Yang, S. Feng, J. Li, W. Liu, Y. Shen and X. Tian, *Coord. Chem. Rev.*, 2023, **475**, 214898.
75 M. G. Kibria, H. P. T. Nguyen, K. Cui, S. Zhao, D. Liu, H. Guo, M. L. Trudeau, S. Paradis, A.-R. Hakima and Z. Mi, *ACS Nano*, 2013, **7**, 7886–7893.
76 K. Liu, B. Zhang, J. Zhang, W. Lin, J. Wang, Y. Xu, Y. Xiang, T. Hisatomi, K. Domen and G. Ma, *ACS Catal.*, 2022, **12**, 14637–14646.
77 S. Guo, Z. Deng, M. Li, B. Jiang, C. Tian, Q. Pan and H. Fu, *Angew. Chem., Int. Ed.*, 2016, **55**, 1830–1834.
78 R. Wang, X. Wang, X. Li, L. Pei, X. Gu and Z. Zheng, *Int. J. Hydrogen Energy*, 2021, **46**, 197–208.
79 M. Bernareggi, G. L. Chiarello, G. West, M. Ratova, A. M. Ferretti, P. Kelly and E. Selli, *Catal. Today*, 2019, **326**, 15–21.
80 G. L. Chiarello, M. H. Aguirre and E. Selli, *J. Catal.*, 2010, **273**, 182–190.
81 T. A. Kandiel, R. Dillert, L. Robben and D. W. Bahnemann, *Catal. Today*, 2011, **161**, 196–201.
82 L. Zhao, M. Tang, F. Wang and X. Qiu, *Fuel*, 2023, **331**, 125748.
83 D. S. Muggli, J. T. McCue and J. L. Falconer, *J. Catal.*, 1998, **173**, 470–483.
84 H. Lu, J. Zhao, L. Li, L. Gong, J. Zheng, L. Zhang, Z. Wang, J. Zhang and Z. Zhu, *Energy Environ. Sci.*, 2011, **4**, 3384.
85 B. Rusinque, S. Escobedo and H. de Lasa, *Catalysts*, 2022, **12**, 113.
86 B. Rusinque, S. Escobedo and H. de Lasa, *Catalysts*, 2021, **11**, 405.
87 Y. Li, Y.-K. Peng, L. Hu, J. Zheng, D. Prabhakaran, S. Wu, T. J. Puchtler, M. Li, K.-Y. Wong, R. A. Taylor and S. C. E. Tsang, *Nat. Commun.*, 2019, **10**, 4421.
88 D. I. Kondarides, V. M. Daskalaki, A. Patsoura and X. E. Verykios, *Catal. Lett.*, 2008, **122**, 26–32.
89 S. Escobedo, B. Rusinque and H. de Lasa, *Ind. Eng. Chem. Res.*, 2019, **58**, 22225–22235.
90 N. Kunthakudee, T. Puangpetch, P. Ramakul, K. Serivalsatit and M. Hunsom, *Int. J. Hydrogen Energy*, 2022, **47**, 23570–23582.
91 W. Feng, L. Zhang, Y. Zhang, Y. Yang, Z. Fang, B. Wang, S. Zhang and P. Liu, *J. Mater. Chem. A*, 2017, **5**, 10311–10320.

92 D. Gunawan, C. Y. Toe, P. Kumar, J. Scott and R. Amal, *ACS Appl. Mater. Interfaces*, 2021, **13**, 49916–49926.
93 M. A. Esteves, F. Fresno, V. R. Fernandes, F. E. Oropeza, V. A. de la Peña O'Shea and C. M. Rangel, *Catal. Today*, 2021, **380**, 41–52.
94 M. C. Herrera-Beurnio, F. J. López-Tenllado, J. Hidalgo-Carrillo, J. Martín-Gómez, R. Estévez, F. J. Urbano and A. Marinas, *Catal. Today*, 2024, **430**, 114548.
95 S. Adhikari, S. D. Fernando and A. Haryanto, *Energy Convers. Manage.*, 2009, **50**, 2600–2604.
96 K. E. Sanwald, T. F. Berto, W. Eisenreich, O. Y. Gutiérrez and J. A. Lercher, *J. Catal.*, 2016, **344**, 806–816.
97 A. K. Wahab and H. Idriss, *Int. J. Hydrogen Energy*, 2024, **52**, 159–171.
98 N. Skillen, K. Ralphs, D. Craig, S. McCalmont, A. F. V. Muzio, C. O'Rourke, H. Manyar and P. K. J. Robertson, *J. Chem. Technol. Biotechnol.*, 2020, **95**, 2619–2627.
99 M. Yasuda, T. Matsumoto and T. Yamashita, *Glycerine Production and Transformation – An Innovative Platform for Sustainable Biorefinery and Energy*, IntechOpen, 2019.
100 S. D. Tristantini, Valentina and M. Ibadurrohman, *Int. J. Energy Res.*, 2013, **37**, 1372–1381.
101 C. Wang, X. Cai, Y. Chen, Z. Cheng, X. Luo, S. Mo, L. Jia, R. Shu, P. Lin, Z. Yang, S. Sun, E. Pu and Y. Shen, *Int. J. Hydrogen Energy*, 2017, **42**, 17063–17074.
102 V. Gombac, L. Sordelli, T. Montini, J. J. Delgado, A. Adamski, G. Adami, M. Cargnello, S. Bernal and P. Fornasiero, *J. Phys. Chem. A*, 2010, **114**, 3916–3925.
103 A. Ruiz-Aguirre, J. G. Villachica-Llamosas, M. I. Polo-López, A. Cabrera-Reina, G. Colón, J. Peral and S. Malato, *Energy*, 2022, **260**, 125199.
104 N. Luo, T. Montini, J. Zhang, P. Fornasiero, E. Fonda, T. Hou, W. Nie, J. Lu, J. Liu, M. Heggen, L. Lin, C. Ma, M. Wang, F. Fan, S. Jin and F. Wang, *Nat. Energy*, 2019, **4**, 575–584.
105 H. Harada, T. Sakata and T. Ueda, *J. Phys. Chem.*, 1989, **93**, 1542–1548.
106 T. Montini, V. Gombac, J. J. Delgado, A. M. Venezia, G. Adami and P. Fornasiero, *Inorg. Chim. Acta*, 2021, **520**, 120289.
107 R. Kumar, G. Swain and S. Dutta, *Fuel*, 2024, **360**, 130555.
108 X. Wang, H. Yu, L. Yang, L. Shao and L. Xu, *Catal. Commun.*, 2015, **67**, 45–48.
109 W. Zhang, Y. Wang, Z. Wang, Z. Zhong and R. Xu, *Chem. Commun.*, 2010, **46**, 7631.
110 X. Zong, G. Wu, H. Yan, G. Ma, J. Shi, F. Wen, L. Wang and C. Li, *J. Phys. Chem. C*, 2010, **114**, 1963–1968.
111 C. Li, H. Wang, S. B. Naghadeh, J. Z. Zhang and P. Fang, *Appl. Catal., B*, 2018, **227**, 229–239.
112 X. Zhang, L. Yu, C. Zhuang, T. Peng, R. Li and X. Li, *ACS Catal.*, 2014, **4**, 162–170.
113 L. Yu, X. Zhang, C. Zhuang, L. Lin, R. Li and T. Peng, *Phys. Chem. Chem. Phys.*, 2014, **16**, 4106.
114 J. Wang, D. Liu, Q. Liu, T. Peng, R. Li and S. Zhou, *Appl. Surf. Sci.*, 2019, **464**, 255–261.
115 J. Wang, Y. Zheng, T. Peng, J. Zhang and R. Li, *ACS Sustainable Chem. Eng.*, 2017, **5**, 7549–7556.
116 A. Speltini, M. Sturini, F. Maraschi, D. Dondi, A. Serra, A. Profumo, A. Buttafava and A. Albini, *Int. J. Hydrogen Energy*, 2014, **39**, 11433–11440.
117 Q. Cheng, Y.-J. Yuan, R. Tang, Q.-Y. Liu, L. Bao, P. Wang, J. Zhong, Z. Zhao, Z.-T. Yu and Z. Zou, *ACS Catal.*, 2022, **12**, 2118–2125.
118 P. Wang, Y. Yuan, Q. Liu, Q. Cheng, Z. Shen, Z. Yu and Z. Zou, *ChemSusChem*, 2021, **14**, 2860–2865.
119 Z.-X. Huang, C. Ma, F.-G. Zhang, Q. Cheng, Q.-Y. Liu, Y.-J. Yuan and X. Zhang, *J. Mater. Chem. A*, 2023, **11**, 7488–7497.
120 D. Jing, H. Liu, X. Zhang, L. Zhao and L. Guo, *Energy Convers. Manage.*, 2009, **50**, 2919–2926.
121 M. Liu, L. Wang, G. (Max) Lu, X. Yao and L. Guo, *Energy Environ. Sci.*, 2011, **4**, 1372.
122 V. M. Daskalaki, M. Antoniadou, G. Li Puma, D. I. Kondarides and P. Lianos, *Environ. Sci. Technol.*, 2010, **44**, 7200–7205.
123 H. Yan, J. Yang, G. Ma, G. Wu, X. Zong, Z. Lei, J. Shi and C. Li, *J. Catal.*, 2009, **266**, 165–168.
124 S. Yang, K. Wang, Q. Chen and Y. Wu, *J. Mater. Sci. Technol.*, 2024, **175**, 104–114.
125 Y. Fan, S. Yu, Y. Wang, Y. Xie and X. Qiu, *Sep. Purif. Technol.*, 2024, **335**, 126243.
126 T. Fei, C. Qin, Y. Zhang, G. Dong, Y. Wang, Y. Zhou and M. Cui, *Int. J. Hydrogen Energy*, 2021, **46**, 20481–20491.
127 J. Fang, F. Sun, A. Kheradmand, H. Xu, H. Dong, X. Yi, H. Hong and X. Liu, *Fuel*, 2023, **353**, 129277.
128 J. Huang, Y. Lu, H. Zhang, L. Shangguan, Z. Mou, J. Sun, S. Sun, J. He and W. Lei, *Chem. Eng. J.*, 2021, **405**, 126685.
129 D. Liu, C. Zhang, J. Shi, Y. Shi, T. T. T. Nga, M. Liu, S. Shen and C. Dong, *Small*, 2024, **20**, 2310289.
130 L. Mao, B. Zhai, J. Shi, X. Kang, B. Lu, Y. Liu, C. Cheng, H. Jin, E. Lichtfouse and L. Guo, *ACS Nano*, 2024, **18**, 13939–13949.
131 K. Takanabe, K. Kamata, X. Wang, M. Antonietti, J. Kubota and K. Domen, *Phys. Chem. Chem. Phys.*, 2010, **12**, 13020.
132 J. Xu, Y. Li, S. Peng, G. Lu and S. Li, *Phys. Chem. Chem. Phys.*, 2013, **15**, 7657.
133 F. Yu, Z. Wang, S. Zhang, H. Ye, K. Kong, X. Gong, J. Hua and H. Tian, *Adv. Funct. Mater.*, 2018, **28**, 1804512.
134 J. Xu, Y. Li and S. Peng, *Int. J. Hydrogen Energy*, 2015, **40**, 353–362.
135 Q. Liu, J. Wang, D. Liu, R. Li and T. Peng, *J. Power Sources*, 2018, **396**, 57–63.
136 Z. Cheng, W. Fang, T. Zhao, S. Fang, J. Bi, S. Liang, L. Li, Y. Yu and L. Wu, *ACS Appl. Mater. Interfaces*, 2018, **10**, 41415–41421.